Article

Albumin orchestrates a natural host defence mechanism against mucormycosis

https://doi.org/10.1038/s41586-025-09882-3

Received: 12 November 2024

Accepted: 7 November 2025

Published online: 7 January 2026

Open access

Check for updates

Antonis Pikoulas[1,23], Ioannis Morianos[1,2,23], Vassilis Nidris[1,2,23], Rania Hamdy[3], Evangelia Intze[1], Ángeles López-López[4], Maria Moran-Garrido[4], Valliappan Muthu[5], Maria Halabalaki[6], Varvara Papaioanou[6], Maria Papadovasilaki[2], Irene Kyrmizi[1,2], Yiyou Gu[7], Sandra M. Camunas-Alberca[4], Robina Aerts[8], Toine Mercier[8], Yuri Vanbiervliet[8], Sung-Yeon Cho[9], Amy Spallone[9], Ying Jiang[9], Dimitrios Samonakis[1], Efstathios Kastritis[10], Carlos Lax[11], Maria Tzardi[1], Aristides Eliopoulos[10], Konstantina Georgila[10], Agostinho Carvalho[12,13], Oliver Kurzai[14,15], Shivaprakash Mandya Rudramurthy[16], Caroline Elie[17,18], Fanny Lanternier[19], Kyriakos Petratos[2,24], Victoriano Garre[11], Elias Drakos[1], Johan Maertens[8], Vincent M. Bruno[20], Dimitrios P. Kontoyiannis[9], Coral Barbas[4], Sameh S. M. Soliman[3,21], Ashraf S. Ibrahim[7,22] & Georgios Chamilos[1,2] ✉

Mucormycosis is an emerging, life-threatening human infection caused by Mucorales fungi[1–3]. Metabolic disorders uniquely predispose an ever-expanding group of patients to mucormycosis through poorly understood mechanisms[1,2,4,5], suggesting that uncharacterized host metabolic effectors may confer protective immunity against this infection. Here we uncover a master regulatory role of albumin in host defence against Mucorales through the modulation of fungal pathogenicity. Our initial studies identified severe hypoalb uminaemia as a prominent metabolic abnormality and an independent biomarker of poor mucormycosis outcome across three distinct cohorts of patients with mucormycosis. Notably, purified albumin selectively inhibits Mucorales growth among a range of pathogens, and albumin-deficient mice display susceptibility specifically to mucormycosis. The antifungal activity of albumin is mediated by the release of bound free fatty acids (FFAs). Albumin prevents FFA oxidation, which otherwise abolishes their antifungal properties, and sera from patients with mucormycosis display high levels of oxidized FFAs. Physiologically, albumin-bound FFAs suppress the expression of key virulence factors by inhibiting protein synthesis, the reby rendering Mucorales avirulent in vivo. Overall, we identify a host defence mechanism that directs the pathogen to suppress its pathogenicity program in response to unfavourable metabolic cues regulated by albumin. These findings have major implications for the pathogenesis and management of mucormycosis.

Mucorales fungi cause mucormycosis—an emerging, life-threatening, opportunistic infection with limited therapeutic options and incompletely understood pathogenesis[1,6,7]. The overall mortality of mucormycosis exceeds 50% and approaches 100% in patients with disseminated disease[1]. The clinical hallmark of mucormycosis is massive tissue necrosis induced by the fungus, which impedes antifungal agents from reaching the sites of infection and often necessitates radical, disfiguring surgery to control the disease[1,8]. In contrast to other fungal infections, mucormycosis predominantly affects an ever-expanding group of patients with metabolic abnormalities through incompletely characterized mechanisms[1,4,5]. Specifically, poorly controlled diabetes mellitus (DM), acidosis, acquired iron overload syndromes, malnutrition and immunometabolic dysregulation induced by COVID-19 uniquely predispose individuals to the development of mucormycosis[1–4,6,8]. Thus, uncharacterized metabolic host defence mechanisms may confer protective immunity against mucormycosis.

From the pathogen perspective, Mucorales senses cues in the tissue environment, triggering the expression of virulence factors that transform these saprophytic organisms into rapidly invasive and potentially lethal pathogens[1]. Specifically, the production of the potent mycotoxin mucoricin during Mucorales hyphae growth[9] induces extensive tissue necrosis, whereas the binding of CotH invasins to specific host receptors promotes angioinvasion and fungal dissemination[10–12]. Notably, germinating spores of Mucorales evade phagocytosis and induce acute lethality within 24 h of pulmonary infection in immunocompetent mice[13]. Thus, it is essential to identify metabolic host effectors that prevent extracellular growth and modulate Mucorales pathogenicity during the early stages of infection.

Albumin selectively inhibits Mucorales

Human serum has important inhibitory effects against Mucorales, which remain molecularly unexplored[14,15]. We found that, compared

A list of affiliations appears at the end of the paper.

with sera from healthy individuals, the ability of sera from patients with mucormycosis to inhibit hyphal growth of a clinical isolate of *Rhizopus arrhizus* var. *delemar* (hereafter, *R. delemar*) is almost completely lost (Fig. 1a). Albumin, the most abundant serum protein, regulates important physiological functions intravascularly, in the interstitial space, and on mucosal surfaces[16]. Furthermore, severe hypoalbuminaemia is a common finding in patients with diverse immunometabolic abnormalities predisposing for mucormycosis[2,5,17]. We therefore decided to comprehensively evaluate the physiological function of albumin against Mucorales.

We initially explored the associations between serum albumin levels and susceptibility to the development of pulmonary mucormycosis and its outcome in contemporaneous high-risk patients with haematological malignancy at a major tertiary care cancer centre in the United States (Supplementary Table 1). Notably, most patients who developed pulmonary mucormycosis had significantly lower albumin levels at diagnosis compared with control patients matched for the underlying disease who developed bacterial pneumonia or pneumonia caused by the major airborne human fungal pathogen *Aspergillus fumigatus* (Fig. 1b). Furthermore, patients with mucormycosis and very low albumin levels (≤2.5 g dl^{-1}) had significantly lower survival rates compared with other patients with mucormycosis (Fig. 1c). These findings were independently validated through an analysis of serum albumin levels in a cohort of patients with pulmonary mucormycosis in a tertiary care centre from the Postgraduate Institute of Medical Education and Research (PGIMER), Chandigarh, India (Fig. 1c and Supplementary Table 1), who had DM and COVID-19 as main underlying risk factors, and a published cohort of patients with mucormycosis from France (Ambizygo Study[18]) who had different risk factors (Fig. 1c). Notably, multivariate survival analysis identified severe hypoalbuminaemia (≤2.5 g dl^{-1}) as an independent predictor of poor outcome across all three clinical cohorts of patients with mucormycosis (Extended Data Tables 1–3).

We next analysed the functional relationship between the serum albumin concentration and antifungal activity in patients at high risk for mucormycosis. Notably, we detected a significant association between the degree of hypoalbuminaemia and the loss of inhibitory activity of serum against *R. delemar* hyphal formation in prospectively collected sera from patients with liver cirrhosis or haematological malignancy (Extended Data Fig. 1a and Supplementary Table 1).

To account for potential confounders related to the underlying disease, we performed albumin depletion in sera from healthy individuals using affinity chromatography[19]. Equilibration of Cibacron Blue chromatography columns was achieved with concentrated serum filtrate previously passed through a 50 kDa centrifugal filter unit, to ensure that the albumin-depleted flow-through was not diluted for other serum proteins. We assessed the effect of albumin depletion on the activity of serum against *R. delemar* and another major human respiratory fungal pathogen *A. fumigatus*[7]. Notably, albumin depletion resulted in a significant loss of antifungal activity of the serum selectively against *R. delemar* but not against *A. fumigatus* (Fig. 1d).

We next purified human albumin from the sera of healthy volunteers to directly evaluate its antifungal activity against Mucorales using a protocol based on affinity column chromatography[19] (Fig. 1e and Extended Data Fig. 1b). We found no evidence of transferrin, a serum iron-transferring protein with important role in nutritional immunity against Mucorales[20], in the albumin-containing eluted fractions by western blot analysis (Extended Data Fig. 1c). Notably, purified human albumin dissolved at physiological concentrations (around 3.5 g dl^{-1}) in liquid culture medium had potent activity against *R. delemar* (Fig. 1f), an effect that was not observed with comparable concentrations of human IgG (Extended Data Fig. 1d). Moreover, purified albumin from different sources, including commercially available bovine serum albumin (BSA) and human serum albumin (HSA) used for therapeutic applications, inhibited Mucorales growth when added at physiologically relevant concentrations in culture medium (Fig. 1g,h). Notably, we found that albumin specifically blocks filamentous (hyphal) growth of Mucorales after the initial stage of isotropic growth (swelling) of fungal spores (Extended Data Fig. 2a). The antifungal activity of albumin was fully reversible after culture of inhibited Mucorales spores in fresh medium without albumin (Extended Data Fig. 2b). Albumin selectively inhibited a wide range of clinical isolates of Mucorales species at physiological serum concentrations (4.5 g dl^{-1}), whereas it showed no significant activity against other major human bacterial or fungal pathogens (Fig. 1i and Extended Data Fig. 2c). Collectively, these results reveal the specialized activity of albumin against Mucorales and identify severe hypoalbuminaemia as an independent biomarker of poor outcome of mucormycosis.

Albumin-bound FFAs inhibit Mucorales

To examine whether the inhibitory activity of albumin requires direct interaction of the protein with fungal cells, we filtered culture medium containing inhibitory concentrations of albumin (4.5 g dl^{-1}) and assessed the antifungal activity of the culture filtrate (flow-through). Notably, we found that the flow-through of albumin retains full inhibitory activity against *R. delemar* (Extended Data Fig. 3a). Nutritional immunity is an essential host defence mechanism against Mucorales[1,13]. In view of the ability of albumin to bind a wide range of compounds, endogenous molecules, iron and other transition metals[21], we investigated the possibility that albumin inhibits Mucorales through depletion of essential nutrients from the culture medium. We therefore analysed the components of regular RPMI culture medium and found that the presence of albumin resulted in a significant reduction in the concentration of certain amino acids (Extended Data Fig. 3b and Supplementary Table 2). However, supplementation experiments with amino acids and different combinations of nutrients contained in RPMI medium did not affect the inhibitory activity of albumin flow-through against *R. delemar* (Extended Data Fig. 3c).

We next considered the possibility that the release of an inhibitory molecule bound to albumin could account for the antifungal activity of the albumin-rich culture filtrate. Serum albumin acts as the main shuttle of non-esterified middle- and long-chain fatty acids (FFAs) in extracellular fluids[22] and FFAs possess antimicrobial properties[23]. We therefore performed fractionation of lipid-containing elutions from a BSA-containing culture filtrate and functionally characterized the inhibitory activity against *R. delemar*. We identified a fraction with significant inhibitory activity against Mucorales; this fraction contained high amounts of caprylic acid (C8:0) as determined using gas chromatography–mass spectrometry (GC–MS) and electrospray ionization high-resolution MS (ESI-HRMS) analysis (Extended Data Fig. 4a–c). We also confirmed that purified caprylic acid dissolved in ethanol has potent inhibitory activity against Mucorales at concentrations lower than those contained in the BSA filtrate (Extended Data Fig. 4d).

To further explore the physiological relevance of our findings, we performed lipidomic profiling in purified human albumin isolated from healthy donors before and after filtration (Fig. 2a). The albumin filtrate retained full inhibitory activity against Mucorales spores (Fig. 2a) and contained physiological middle- and long-chain FFAs (Fig. 2b and Supplementary Table 3). Furthermore, we found that purified serum FFAs dissolved in ethanol exerted potent anti-Mucorales activity at physiologically relevant concentrations[24] (Fig. 2c). We also found that a broad range of FFAs of various carbon chain lengths and degrees of saturation display potent antifungal activity against Mucorales (Fig. 2d). Importantly, purified human albumin after charcoal treatment for the removal of bound FFAs[25], or commercially available BSA free of fatty acids (FFA-free BSA), had no activity against Mucorales (Fig. 2e). Furthermore, charcoal-treated BSA complexed with physiologically relevant concentrations of oleic acid (OA) dissolved the FFA and fully restored its activity against Mucorales (Fig. 2f). Experiments

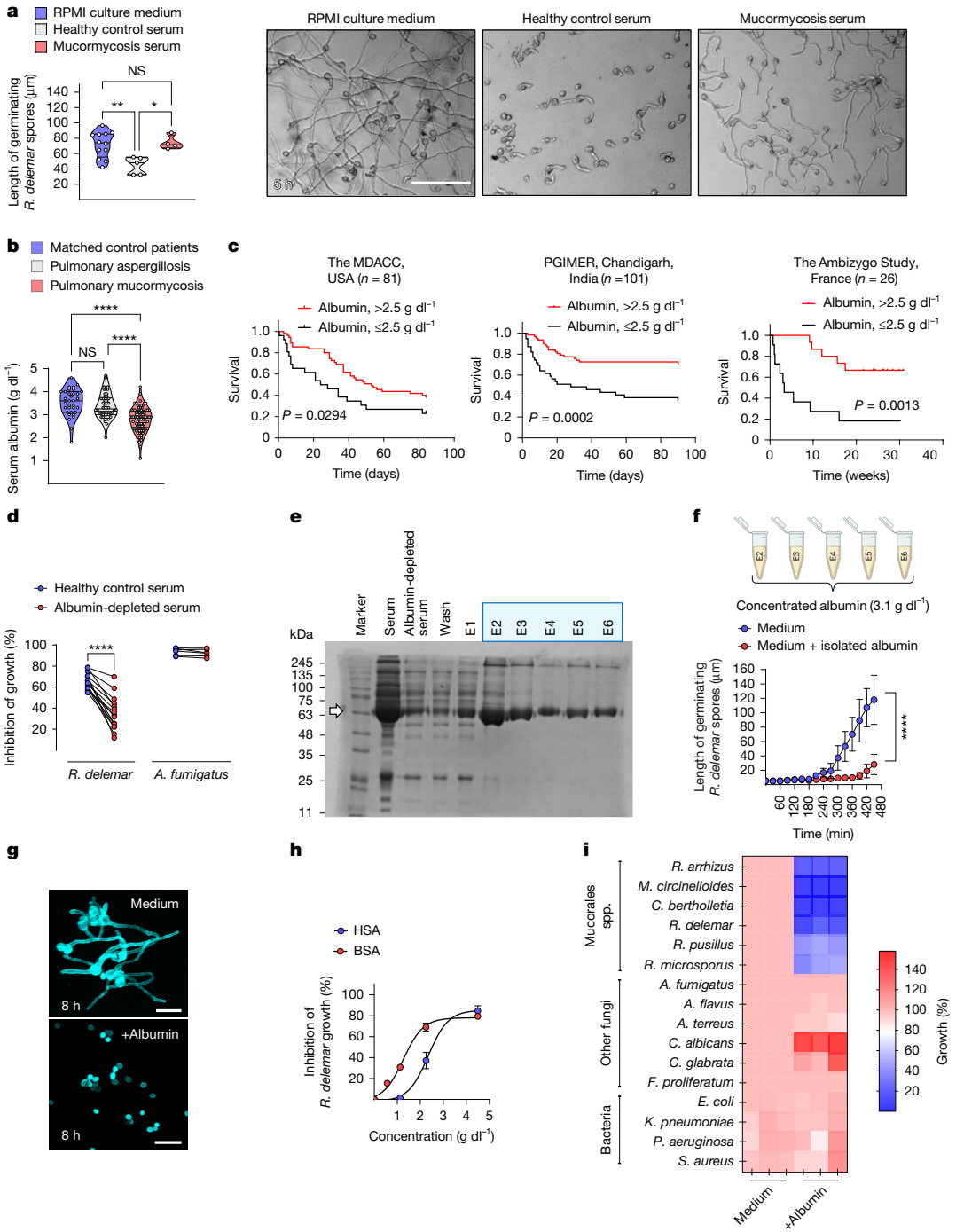

Fig. 1 | Selective antifungal activity of albumin against Mucorales. **a**, The length of germinating *R. delemar* spores cultured for 5 h in RPMI medium ($n = 12$), serum from healthy individuals ($n = 5$) or serum from patients with mucormycosis before initiation of antifungals ($n = 4$). Statistical analysis was performed using one-way analysis of variance (ANOVA) with Tukey's post hoc test; $^{*}P = 0.0213$, $^{**}P = 0.0079$. Representative images are shown. Scale bar, 100 µm. **b**, Serum albumin concentrations at diagnosis in contemporaneously matched controls ($n = 33$), patients with pulmonary aspergillosis ($n = 50$) and patients with mucormycosis ($n = 81$). Statistical analysis was performed using one-way ANOVA with Tukey's post hoc test; NS, not significant ($P = 0.466$). **c**, Kaplan–Meier survival curves for patients with mucormycosis presenting with severe hypoalbuminaemia (≤2.5 g dl^{-1}) compared with all other mucormycosis cases from independent clinical cohorts in the USA ($n = 81$), India ($n = 101$) and France ($n = 26$). Survival differences were assessed using the log-rank (Mantel–Cox) test. MDACC, MD Anderson Cancer Center. **d**, The effect of albumin depletion from human serum of healthy donors on the growth of *R. delemar* ($n = 15$) and *A. fumigatus* ($n = 6$). Statistical analysis was performed using two-sided Wilcoxon matched-pairs signed-rank test; NS, $P = 0.156$. **e**, Coomassie blue staining of intact human serum, albumin-depleted serum and albumin-enriched eluates. Representative of three independent experiments. **f**, Germ-tube elongation of *R. delemar* spores cultured in medium with or without purified HSA, quantified by time-lapse microscopy. $n = 50$–200 spores per timepoint; two independent experiments, performed in triplicate. Data are mean ± s.d. Statistical analysis was performed using two-way ANOVA with Sidak's multiple-comparisons test. **g**, Representative images of Calcofluor White (CFW)-stained *R. delemar* spores after 8 h of culture in medium with or without HSA. Scale bars, 50 µm. **h**, Inhibition of *R. delemar* growth by increasing concentrations of HSA or BSA. $n = 4$ independent experiments performed in triplicate. Data are mean ± s.d. **i**, Quantification of the growth of different Mucorales species and other pathogens cultured in medium with or without HSA. Representative of three independent experiments in triplicate. Full scientific names are given in the Methods. $^{****}P < 0.0001$ (**b**,**d**,**f**). The diagram in **f** was created using BioRender.

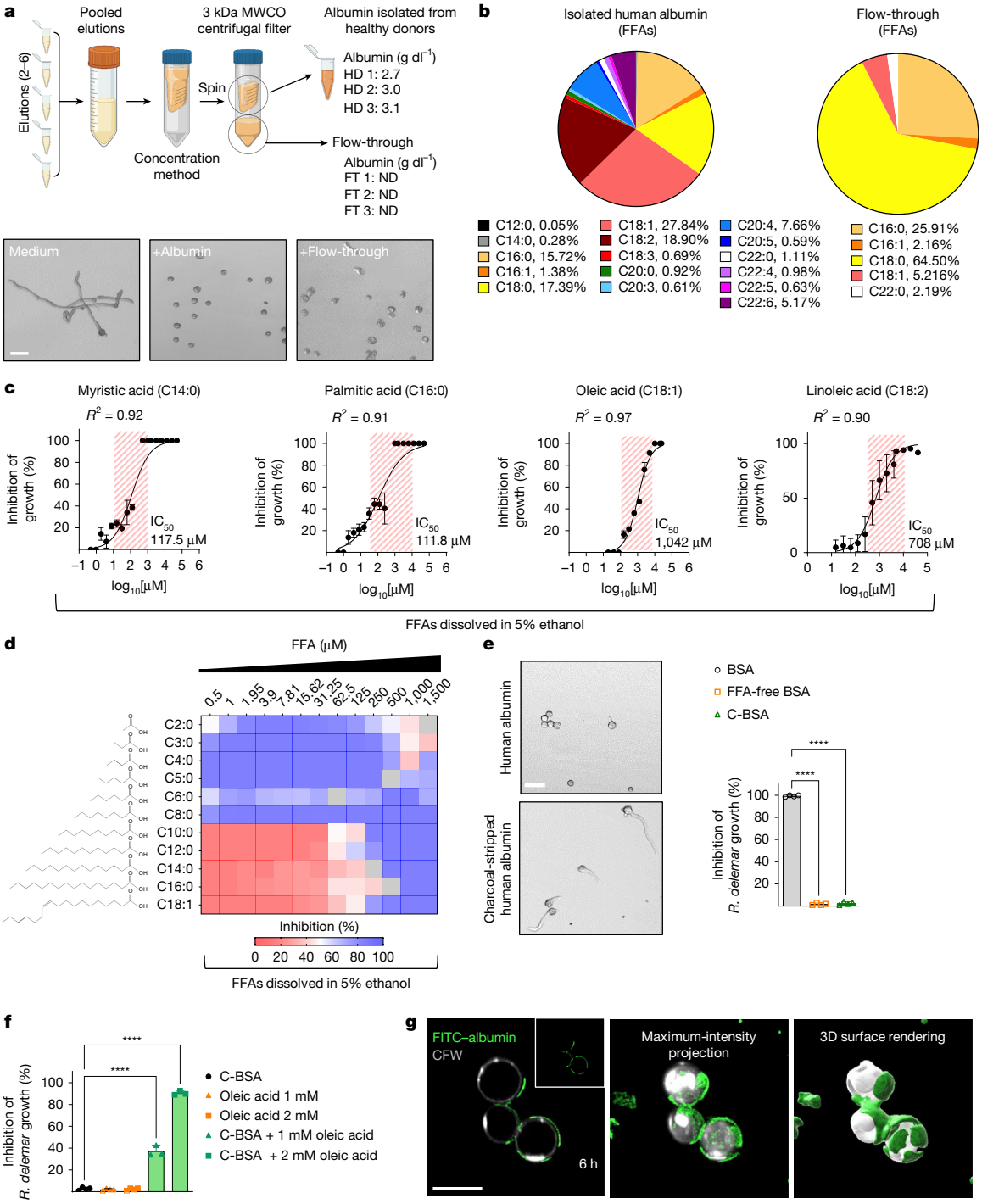

Fig. 2 | Physiological FFAs mediate the antifungal activity of albumin against Mucorales. a, Schematic of the experimental workflow for generating flow-through and isolating albumin from human serum using a 3 kDa molecular weight cut-off (MWCO) centrifugal filter (top). Bottom, representative bright-field images from three independent experiments showing *R. delemar* spores cultured for 5 h in minimal medium alone or in medium supplemented with isolated HSA or albumin flow-through. FT, flow-through; HD, healthy donor; ND, not detectable. Scale bar, 50 µm. **b**, Lipidomic profiling of FFAs in isolated HSA and corresponding flow-through obtained as in **a**. **c**, Antifungal activity of the major serum FFAs against *R. delemar*. The red-striped areas indicate physiological serum concentrations of each FFA. Data are mean ± s.d., representative of $n = 3$ independent experiments. IC_{50}, half-maximum inhibitory concentration. **d**, The dose-dependent inhibitory effect of short-, medium- and long-chain FFAs on *R. delemar* growth. **e**, Representative images of *R. delemar* spores cultured for 5 h in medium supplemented with isolated HSA or charcoal-stripped albumin (left). Scale bar, 50 µm. Right, quantification of *R. delemar* growth inhibition by BSA, FFA-free BSA or charcoal-stripped BSA. $n = 4$ independent experiments, performed in triplicate. Data are mean ± s.d. Statistical analysis was performed using one-way ANOVA with Tukey's multiple-comparison test; NS, $P = 0.574$. **f**, The inhibitory effects of charcoal-stripped BSA, OA or charcoal-stripped BSA reconstituted with OA on *R. delemar* growth. Data are a representative example of $n = 3$ independent experiments, shown as the mean ± s.d., performed in triplicate. Statistical analysis was performed using one-way ANOVA with Tukey's multiple-comparison test. **g**, Representative fluorescence microscopy images from three independent experiments showing CFW-labelled *R. delemar* spores cultured for 6 h in the presence of FITC-labelled albumin, performed in duplicate. Scale bar, 10 µm. ****$P < 0.0001$ (**e**,**f**). The diagram in **a** was created using BioRender.

with fluorescent-labelled albumin further demonstrated that, although albumin avidly binds to the fungal cell wall, it is not internalized by Mucorales spores (Fig. 2g). Collectively, these findings demonstrate that albumin binds to, dissolves, shuttles and facilitates the release of physiological FFAs to optimize their antifungal activity.

Albumin protects FFAs from oxidation

We next performed targeted lipidomic profiling of the sera of patients with mucormycosis and matched controls to analyse the FFA composition and identify abnormalities associated with the loss of antifungal activity in the serum. Notably, we found that the sera of patients with mucormycosis contained a significantly greater proportion of oxidized forms of FFAs than the sera of control patients, who were matched for the underlying disease without infection or those who have been diagnosed with invasive aspergillosis (Fig. 3a and Supplementary Table 3). Furthermore, the sera of patients susceptible to mucormycosis due to underlying cirrhosis or haematological malignancy contained high amounts of oxidized FFAs, which was directly proportional to the severity of hypoalbuminaemia, particularly in cirrhosis (Fig. 3b,c). Importantly, in patients with cirrhosis, the degree of serum FFA oxidation was strongly correlated with the loss of inhibitory activity against Mucorales (Fig. 3d), whereas this association was less pronounced in the sera of patients with haematological malignancy. Collectively, these findings suggested that oxidized FFAs display attenuated activity against Mucorales.

To directly evaluate the antifungal activity of oxidized FFAs, we oxidized OA—a major physiological serum FFA—and assessed the effect on antifungal activity. We found that the oxidation of OA resulted in a greater than 100-fold decrease in its inhibitory activity against *R. delemar* (Fig. 3e). To establish a causal relationship between FFA oxidation and the loss of anti-Mucorales activity in serum, we isolated serum lipids from healthy individuals and assessed the effects of oxidation on their antifungal properties. Importantly, oxidation of serum lipids resulted in a significant decrease in their inhibitory properties against *R. delemar* spores (Fig. 3f).

As FFA oxidation diminishes their uptake by mammalian cells[26], we evaluated the internalization of oxidized FFAs by fungal cells. We initially found that the uptake of a long-chain FFA fluorescent analogue C12-BODIPY by Mucorales spores is energy dependent, as it was abolished at 0 °C (Extended Data Fig. 5a). We next evaluated uptake of C11-BODIPY$^{581/591}$ (hereafter, C11-BODIPY), a ratiometric reporter of lipid peroxidation that shifts its fluorescence after oxidation from red (around 590 nm; reduced) to green (around 510 nm; oxidized)[27], in *R. delemar* spores with or without previous in vitro oxidation. Pre-oxidation almost completely abolished C11-BODIPY uptake by *R. delemar*, as indicated by a marked reduction in both reduced and oxidized fluorescence within fungal cells (Fig. 3g and Extended Data Fig. 5b). Furthermore, we measured OA uptake by *R. delemar* cells by fluorescence labelling with Nile Red lipid dye[28]. Notably, we detected a substantial degree of OA uptake by *R. delemar* spores within a few hours in culture, which was profoundly reduced after OA oxidation (Extended Data Fig. 5c,d).

Given the well-established antioxidant properties of albumin[21], we reasoned that the binding of FFAs to albumin can protect them from oxidation. We therefore performed chemical oxidation of OA dissolved in ethanol or after complexation with albumin and assessed the degree of oxidation. We found that albumin significantly protected OA from oxidation (Fig. 3h) and retained its antifungal properties against Mucorales (Fig. 3i).

Albumin glycation induced by DM, a major predisposing factor for mucormycosis[1], results in the dissociation of FFAs from their binding sites and increased oxidation[29] We therefore performed in vitro glycation of albumin (BSA) and assessed its ability to inhibit Mucorales. BSA glycation led to near-complete dissociation of bound FFA (Fig. 3j and Extended Data Fig. 5e–g), resulting in significant loss of albumin antifungal activity (Fig. 3k). Collectively, these studies reveal that albumin protects FFAs from oxidation, which results in the loss of their antifungal activity against Mucorales. Moreover, we identified FFA oxidation as a prominent abnormality in mucormycosis sera.

FFAs target pathogenicity of Mucorales

We next investigated the physiological importance of albumin during in vivo infection with Mucorales after pulmonary infection of immunocompetent mice with swollen fungal spores[13]. Specifically, we allowed dormant spores of *R. delemar* to grow in culture medium with or without physiological concentrations (4.5 g dl^{-1}) of albumin for around 4 h and performed intratracheal (i.t.) infection of the mice (Fig. 4a). We found that albumin pre-exposure rendered *R. delemar* spores almost completely avirulent in vivo (Fig. 4b). Notably, pre-exposure to albumin did not inhibit the in vivo germination of Mucorales during the early stages of infection in the lungs (Extended Data Fig. 6a). Instead, albumin pre-exposure completely abrogated massive tissue necrosis and tissue invasion induced by germinating fungal spores, as evidenced by staining for active caspase-3 in sections of the lung (Fig. 4c), and lung fungal burden determined by quantitative PCR (qPCR; Fig. 4d) and histopathology (Fig. 4e). These findings suggest a predominant effect of albumin in attenuating the virulence of Mucorales.

We next performed RNA-sequencing (RNA-seq) analysis during the in vitro growth of *R. delemar* to examine the molecular mechanism of action of albumin on the pathogenicity program of the fungus (Fig. 4f). Volcano plot analysis revealed that albumin treatment differentially modulated the expression of a large number of genes within 3 h (Fig. 4g). Enrichment analysis (Gene Ontology (GO) (Fig. 4h) and KEGG (Extended Data Fig. 6b,c and Supplementary Table 3)) showed broad downregulation of protein-synthesis pathways, accompanied by induction of oxidative stress responses and lipid metabolism. To test whether albumin-bound FFAs directly impact fungal protein synthesis, we measured global translation in *R. delemar* using an assay based on incorporation of *O*-propargyl-puromycin (OP-puro) into nascent polypeptide chains, detected by click-chemistry with a fluorescent azide[30]. Both BSA and purified caprylic acid almost completely inhibited OP-puro incorporation in germinating *R. delemar* spores within 2 h of treatment (Fig. 4i,j). In view of the pronounced inhibitory effect of albumin-bound FFAs on protein synthesis, we analysed the transcriptional response of all characterized virulence factors of Mucorales, including CotH invasins[1,10], the mycotoxin mucoricin[9] and genes regulating the iron assimilation program of the fungus[1]. Notably, we identified mucoricin and CotH3 invasin[10] as the genes most significantly downregulated by albumin at 6 h of *R. delemar* growth (Fig. 4k). We also found that pre-exposure of Mucorales to the albumin culture filtrate almost completely abolished the expression of mucoricin and CotH3 on the surface of swollen spores, as evidenced by immunostaining (Fig. 4l and Extended Data Fig. 6d); similarly, exposure of *R. delemar* spores to purified FFAs blocked mucoricin protein expression (Extended Data Fig. 6e). Finally, the silencing of mucoricin in *R. delemar* (mucoricin RNA interference (RNAi) strain[9]) resulted in a significant decrease in the pathogenicity of swollen spores after pulmonary infection of immunocompetent mice (Extended Data Fig. 6f). Overall, these results reveal that albumin-bound FFAs inhibit protein synthesis to modulate pathogenicity during in vivo fungal growth.

Albumin deficiency promotes mucormycosis

We next used a humanized model of albumin knockout (KO) transgenic mice to genetically validate the role of albumin in host defence against Mucorales[31]. These transgenic mice are double KO for albumin and the neonatal Fc receptor (FcRn), which regulates the recycling of albumin, and transgenic for human FcRn. The expression of human FcRn results

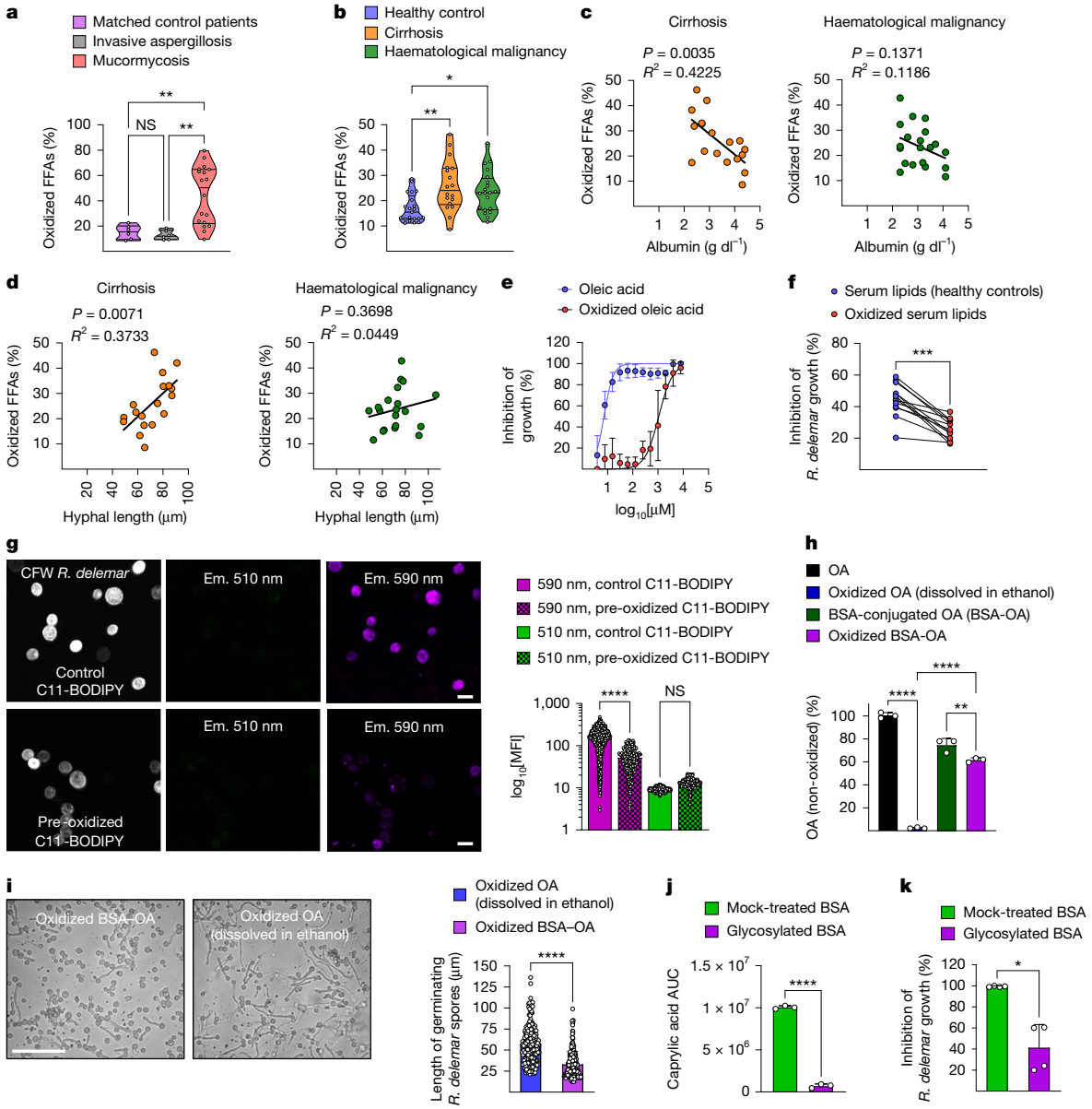

Fig. 3 | Albumin protects FFAs from oxidation and preserves their antifungal activity against Mucorales. a, The relative concentrations of oxidized FFAs in sera from matched control patients ($n = 6$), patients with invasive aspergillosis ($n = 6$) and mucormycosis ($n = 18$). NS, $P = 0.973$; $^{**}P = 0.0061$, $^{**}P = 0.0031$. **b**, The relative concentrations of oxidized FFAs in sera from healthy controls ($n = 21$), patients with cirrhosis ($n = 18$) and patients with haematological malignancies ($n = 20$). NS, $P = 0.576$; $^{*}P = 0.0402$, $^{**}P = 0.0066$. **c**,**d**, Correlation between oxidized serum FFAs and albumin levels (**c**) or antifungal activity (**d**) of sera from patients with cirrhosis ($n = 18$) and haematological malignancies ($n = 20$) against *R. delemar*. Statistical analysis was performed using two-sided linear regression. **e**, Inhibitory effects of increasing concentrations of OA and oxidized OA on *R. delemar* growth. $n = 2$ independent experiments performed in triplicate. Data are mean ± s.d. **f**, Serum lipids from healthy individuals were oxidized and tested for antifungal activity. $n = 13$. Statistical analysis was performed using the two-sided Wilcoxon matched-pairs signed-rank test; $^{***}P = 0.0002$. **g**, CFW-labelled *R. delemar* spores cultured for 3 h with control or pre-oxidized C11-BODIPY (left). Scale bars, 8 μm. Right, quantification of C11-BODIPY mean fluorescence intensity (MFI) at 510 nm and 590 nm ($n = 269$–979 spores, three experiments). NS, $P = 0.769$. Em., emission. **h**, GC–MS analysis of non-oxidized OA in OA and BSA-conjugated OA before and after microwave oxidation. $n = 3$, triplicates. $^{**}P = 0.0041$. **i**, *R. delemar* spores cultured for 5 h with oxidized OA or oxidized BSA–OA. Scale bar, 100 μm. Quantification of germling length is shown. $n = 202$–237 spores, three experiments. Statistical analysis was performed using two-sided Mann–Whitney *U*-tests. **j**, Area under the curve (AUC) quantification of caprylic acid in mock-treated and glycosylated BSA. $n = 3$, triplicates. Statistical analysis was performed using two-sided unpaired *t*-tests. **k**, The inhibitory effects of mock-treated and glycosylated BSA on *R. delemar* growth ($n = 4$, triplicates). Statistical analysis was performed using two-sided Mann–Whitney *U*-tests; $^{*}P = 0.0286$. For **i**–**k**, data are mean ± s.d. For **a**, **b**, **g** and **i**, statistical analysis was performed using one-way ANOVA with Tukey's test. $^{****}P < 0.0001$ (**g**–**j**).

in a prolonged half-life of human albumin following systemic administration[31]. We found that albumin KO ($Alb^{-/-}$) mice were highly susceptible to disseminated and pulmonary *R. delemar* infection (Fig. 5a). However, $Alb^{-/-}$ mice displayed comparable susceptibility to control $Alb^{+/+}$ mice after pulmonary infection with *A. fumigatus* in the neutropenic model of invasive aspergillosis (Fig. 5b and Extended Data Fig. 7a) or disseminated bloodstream infection with *Candida albicans* (Fig. 5c). Importantly, prophylactic or pre-emptive therapeutic administration of purified, FFA-free human albumin fully restored the resistance of $Alb^{-/-}$ mice to pulmonary mucormycosis (Fig. 5d). Histopathological sections

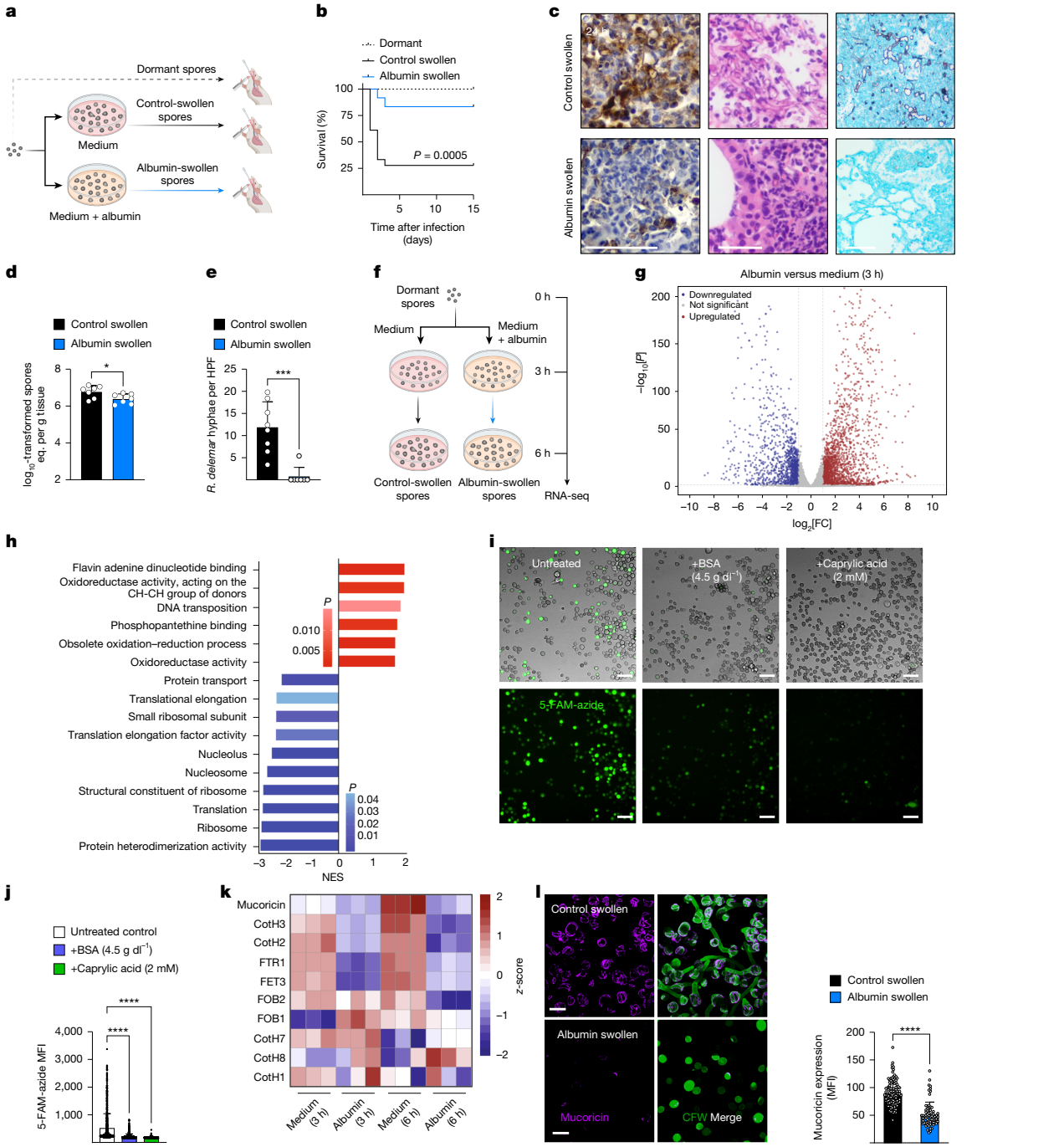

Fig. 4 | Albumin-bound FFAs target Mucorales pathogenicity by inhibiting protein synthesis. a, Schematic of i.t. instillation of dormant or swollen *R. delemar* spores. **b**, Survival of C57BL/6 mice infected i.t. with 2.5×10^6 dormant ($n = 6$), control-swollen ($n = 18$) or albumin-swollen ($n = 12$) spores as in **a**. Statistical significance was determined using the log-rank (Mantel–Cox) test. **c**, Representative lung histopathology on day 1 after infection with control- or albumin-swollen spores, stained for active caspase-3 (left), haematoxylin and eosin (H&E; middle) and Grocott's methenamine silver (GMS; right). Scale bars, 100 µm. **d**, The fungal burden determined by qPCR, expressed as spores per g of lung tissue. $n = 7$ mice. Statistical analysis was performed using a two-sided unpaired *t*-test; $^*P = 0.0331$. eq., equivalent. **e**, Quantification of GMS-stained *R. delemar* hyphae in lung tissue. $n = 8$ control-swollen and $n = 7$ albumin-swollen mice. Statistical analysis was performed using two-sided Mann–Whitney *U*-tests; $^{***}P = 0.0006$. HPF, high-power field. **f**, Workflow of RNA-seq analysis of dormant and swollen spores cultured as in **a** for 3 h and 6 h. **g**, Differentially expressed genes (DEGs) in albumin-swollen versus control-swollen spores. The red and blue dots indicate upregulated and downregulated genes, respectively. FC, fold change. **h**, Enriched GOs among DEGs identified by gene set enrichment analysis after culture of spores in albumin versus medium for 3 h. NES, normalized enrichment score. **i**, Representative fluorescence images of *R. delemar* spores cultured for 5 h in RPMI medium alone or supplemented with BSA (4.5 g dl^{-1}) or caprylic acid (2 mM). Protein synthesis was assessed by OP-puro incorporation and 5-FAM-azide staining. Scale bars, 20 µm. **j**, Quantification of 5-FAM-azide MFI. $n = 943$–$1{,}191$ spores per group, three independent experiments. Statistical analysis was performed using one-way ANOVA with Tukey's test. **k**, Differential mRNA expression of virulence-related genes after incubation in medium with or without albumin for 3 or 6 h. $n = 3$ biologically independent samples. Data show $\log_2$-transformed normalized counts per million (CPM) values. **l**, Confocal images of mucoricin expression in CFW-labelled control- and albumin-swollen *R. delemar* spores after 3 h (left). $n = 107$ control-swollen and $n = 70$ albumin-swollen spores, three experiments. Scale bars, 10 µm. Right, quantification of the mucoricin fluorescence intensity. Statistical analysis was performed using two-sided Mann–Whitney *U*-tests. Data are mean ± s.d. $^{****}P < 0.0001$ (**j**,**l**). The diagrams in **a** and **f** were created using BioRender.

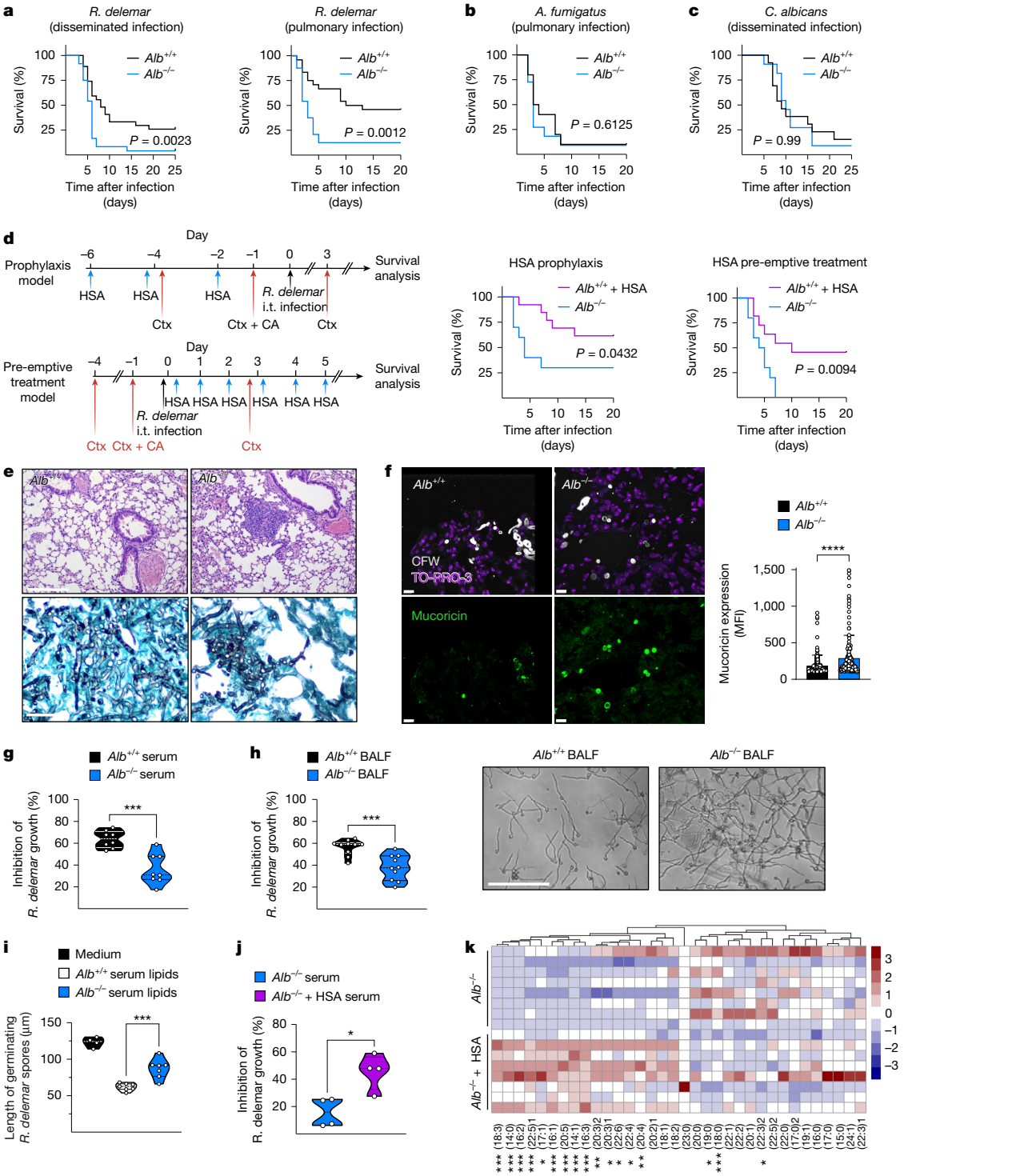

Fig. 5 | Selective susceptibility of albumin-KO mice to mucormycosis. **a**, Survival of $Alb^{+/+}$ and $Alb^{-/-}$ mice that were infected with *R. delemar* intravenously (i.v.) (left; $n = 24–27$; 1×10^5 spores) or i.t (right; $n = 24$; 1×10^6 spores). **b**, Survival of neutropenic $Alb^{+/+}$ and $Alb^{-/-}$ mice infected i.t. with 1×10^6 *A. fumigatus* spores. $n = 11$. **c**, Survival of $Alb^{+/+}$ ($n = 13$) and $Alb^{-/-}$ ($n = 11$) mice infected i.v. with 7.5×10^5 *C. albicans* blastoconidia. **d**, Outline of administration of FFA-free HSA (left). Right, survival of neutropenic $Alb^{-/-}$ mice with or without FFA-free HSA administered before infection ($n = 10–13$) or after 6 h of i.t. infection with 1×10^6 *R. delemar* spores ($n = 10–11$). CA, cortisone acetate; Ctx, cyclophosphamide. For **a**–**d**, statistical analysis was performed using the two-sided log-rank (Mantel–Cox) test. **e**, Representative lung histopathology on day 3 after infection with *R. delemar* in neutropenic $Alb^{+/+}$ and $Alb^{-/-}$ mice. Scale bars, 100 μm. **f**, Representative fluorescence images on mucoricin expression in lung sections from the experiment in **e** (left). Scale bars, 10 μm. Right, quantification of mucoricin fluorescence. $n = 220$ spores per group, three experiments. $^{****}P < 0.0001$. **g**, Inhibitory effect of serum from $Alb^{+/+}$ and $Alb^{-/-}$ mice on *R. delemar* growth ($n = 8$). $^{***}P = 0.0006$. **h**, The inhibitory effect of bronchoalveolar fluid (BALF) from $Alb^{+/+}$ and $Alb^{-/-}$ mice on *R. delemar* growth (left). $n = 8$. $^{***}P = 0.0007$. Right, representative images of spores cultured 5 h in BALF. Scale bar, 100 μm. **i**, The inhibitory effect of serum lipids isolated from $Alb^{+/+}$ and $Alb^{-/-}$ mice on *R. delemar* growth. $n = 7$. Statistical analysis was performed using one-way ANOVA with Tukey's test; $^{***}P = 0.0005$. **j**, The inhibitory effect of serum from $Alb^{-/-}$ mice with or without FFA-free HSA supplemented as in **d**. $n = 4$. $^{*}P = 0.0286$. **k**, Serum FFAs from $Alb^{-/-}$ mice with or without FFA-free HSA supplemented as in **d**. $n = 8$. Statistical analysis was performed using Wilcoxon rank-sum tests. Data are mean ± s.d. For **f**, **g**, **h** and **j**, statistical analysis was performed using two-sided Mann–Whitney *U*-tests. The diagram in **d** was created using BioRender.

of lungs from neutropenic $Alb^{-/-}$ versus $Alb^{+/+}$ mice after pulmonary infection with *R. delemar* revealed invasive fungal growth (Fig. 5e). $Alb^{-/-}$ exhibited a trend toward higher pulmonary fungal burden (Extended Data Fig. 7b) and significantly higher expression of mucoricin on germinating hyphae, as evidenced by immunostaining of the tissue (Fig. 5f). Notably, albumin significantly attenuated mucoricin-induced cytotoxicity in epithelial cells ex vivo (Extended Data Fig. 7c). Sera (Fig. 5g) and bronchoalveolar fluid (Fig. 5h) obtained from $Alb^{-/-}$ mice exhibited significant loss of inhibitory activity against *R. delemar* growth, and serum lipids from these mice were less inhibitory towards Mucorales (Fig. 5i). Lipidomic analyses of serum FFAs revealed a significantly lower amount of non-oxidized FFAs in $Alb^{-/-}$ mice compared with in $Alb^{+/+}$ mice, particularly at 72 h of infection (Extended Data Fig. 7d,e and Supplementary Table 3), consistent with previous reports[32]. $Alb^{-/-}$ sera also contained a significantly higher proportion of oxidized FFAs, although their absolute levels were comparable to those in $Alb^{+/+}$ mice (Extended Data Fig. 7d,f and Supplementary Table 3). Consistent with these findings, albumin administration restored the inhibitory activity of $Alb^{-/-}$ serum (Fig. 5j) and led to a significant increase in a subset of non-oxidized serum FFAs (Fig. 5k). These results provide definitive evidence of the master regulatory role of albumin in host defence against Mucorales.

Discussion

Our initial studies revealed an interesting association between low albumin levels and the development of mucormycosis in high-risk patients with haematological malignancies. Furthermore, severe hypoalbuminaemia independently predicted poor outcome of mucormycosis across patient cohorts with distinct risk factors, on three different continents. These compelling findings are consistent with previous reports on the increased susceptibility of patients with disease-related malnutrition to mucormycosis[1,2,5,17,33,34]. Given the lack of host biomarkers for prognostication of mucormycosis, albumin levels should be further investigated as a readily available, inexpensive and universal biomarker to stratify patients at risk and predict infection outcome.

Susceptibility studies after HSA depletion and purification provided unambiguous evidence of the specialized inhibitory activity of albumin against Mucorales. Functional analysis of lipid-containing fractions and lipidomic profiling of the albumin culture filtrate revealed that the antifungal activity of albumin is exclusively mediated by the release of bound physiological FFAs. The antimicrobial properties of naturally occurring FFAs have long been recognized[23,35,36], particularly at epithelial surfaces where they reach concentrations that are orders of magnitude greater than those in serum and other extracellular fluids[36–39]. However, a host-protective role of albumin-bound FFAs has not been previously demonstrated. By contrast, bacterial pathogens exploit albumin as a source of FFAs to support growth[40], and albumin can reprogram *C. albicans* metabolism independently of FFAs to promote pathogenicity ex vivo[41]. Consistent with these observations, we found that albumin lacks antimicrobial activity against human pathogens other than Mucorales.

Further experiments demonstrated that albumin has an essential role in dissolving, shuttling and protecting bound FFAs from oxidation. Notably, we also found that oxidized FFAs are not internalized by fungal cells and lose their antifungal properties. Whether the systemic antioxidant properties of albumin[42] extend to other serum lipids not directly bound to it remains to be determined. Collectively, these unique properties of albumin promote FFA accumulation within Mucorales spores and result in the inhibition of fungal growth. Moreover, the extensive FFA oxidation in the sera of patients with mucormycosis is associated with the loss of antifungal activity, highlighting the physiological importance of albumin in host defence against Mucorales. Finally, the glycation of albumin, a modification associated with reduced FFA-binding capacity in patients with poorly controlled DM[29], abolished its inhibitory activity against Mucorales due to dissociation of bound FFAs, providing mechanistic insights into the heightened mucormycosis risk in this patient population.

Notably, pre-exposure to albumin almost completely abrogated virulence of germinating *R. delemar* spores during in vivo infection of immunocompetent mice, as a result of inhibition of protein synthesis and the transcriptional downregulation of key virulence factors, especially CotH3 invasin[10] and the potent mycotoxin mucoricin[9]. Future work will elucidate the precise molecular mechanism by which FFAs selectively inhibit protein synthesis in Mucorales.

In concordance with human mucormycosis cohorts, studies of disseminated and pulmonary infection by Mucorales and other major human fungal pathogens in albumin-KO humanized mice provided definitive evidence for a non-redundant, specialized role of albumin in immunity against Mucorales. The reversal of susceptibility in albumin-KO mice and the restoration of serum antifungal activity after albumin supplementation, provide strong rationale for correcting hypoalbuminaemia as (1) a low-cost preventive strategy in high-risk patients and (2) an adjunct therapeutic modality in established mucormycosis. The therapeutic value albumin in mucormycosis warrants evaluation in prospective clinical studies.

Our findings support a pathogenetic model of mucormycosis (Extended Data Fig. 7g) that explains the unique epidemiological features of this disease. Metabolic abnormalities that result in severe hypoalbuminaemia or chemical modifications that impair binding capacity of the protein for FFAs (such as glycation) lead to increased FFA oxidation and loss of their antifungal activity. Systemic oxidative stress induced by hyperinflammation, comorbidities or iron overload may further enhance FFA oxidation and susceptibility to mucormycosis[1]. Hypoalbuminaemia, a biomarker of poor outcome in multiple infectious[43,44] and non-infectious[45,46] diseases, probably reflects the broader immunometabolic functions of albumin and its bound FFAs. Defining the mechanistic basis and therapeutic potential of these interactions represents an important avenue for future research.

Finally, our work provides interesting cues on the mechanisms of selection pressure that account for the enigmatic evolution of albumin in vertebrates[47], by linking its unique lipid-binding properties with the modulation of the pathogenicity of ubiquitous, toxin-producing phytopathogenic fungi. Collectively, these findings have implications for the immunopathogenesis and therapeutics of an emerging human fungal disease with limited treatment options.

Online content

Any methods, additional references, Nature Portfolio reporting summaries, source data, extended data, supplementary information, acknowledgements, peer review information; details of author contributions and competing interests; and statements of data and code availability are available at https://doi.org/10.1038/s41586-025-09882-3.

1. Alqarihi, A., Kontoyiannis, D. P. & Ibrahim, A. S. Mucormycosis in 2023: an update on pathogenesis and management. *Front. Cell Infect. Microbiol.* **13**, 1254919 (2023).
2. Ribes, J. A., Vanover-Sams, C. L. & Baker, D. J. Zygomycetes in human disease. *Clin. Microbiol. Rev.* **13**, 236–301 (2000).
3. Hoenigl, M. et al. The emergence of COVID-19 associated mucormycosis: a review of cases from 18 countries. *Lancet Microbe* **3**, e543–e552 (2022).
4. Hoenigl, M. et al. COVID-19-associated fungal infections. *Nat. Microbiol.* **7**, 1127–1140 (2022).
5. Muthu, V. et al. Risk factors, mortality, and predictors of survival in COVID-19-associated pulmonary mucormycosis: a multicentre retrospective study from India. *Clin. Microbiol. Infect.* **30**, 368–374 (2024).
6. Baldin, C. & Ibrahim, A. S. Molecular mechanisms of mucormycosis—the bitter and the sweet. *PLoS Pathog.* **13**, e1006408 (2017).
7. Iliev, I. D. et al. Focus on fungi. *Cell* **187**, 5121–5127 (2024).
8. Spellberg, B., Edwards, J. Jr & Ibrahim, A. Novel perspectives on mucormycosis: pathophysiology, presentation, and management. *Clin. Microbiol. Rev.* **18**, 556–569 (2005).
9. Soliman, S. S. M. et al. Mucoricin is a ricin-like toxin that is critical for the pathogenesis of mucormycosis. *Nat. Microbiol.* **6**, 313–326 (2021).
10. Gebremariam, T. et al. CotH3 mediates fungal invasion of host cells during mucormycosis. *J. Clin. Invest.* **124**, 237–250 (2014).

11. Liu, M. et al. The endothelial cell receptor GRP78 is required for mucormycosis pathogenesis in diabetic mice. *J. Clin. Invest.* **120**, 1914–1924 (2010).
12. Alqarihi, A. et al. GRP78 and integrins play different roles in host cell invasion during mucormycosis. *mBio* **11**, e01087-20 (2020).
13. Andrianaki, A. M. et al. Iron restriction inside macrophages regulates pulmonary host defense against *Rhizopus* species. *Nat. Commun.* **9**, 3333 (2018).
14. Gale, G. R. & Welch, A. M. Studies of opportunistic fungi. I. Inhibition of *Rhizopus oryzae* by human serum. *Am. J. Med. Sci.* **241**, 604–612 (1961).
15. Eng, R. H., Corrado, M. & Chin, E. Susceptibility of Zygomycetes to human serum. *Sabouraudia* **19**, 111–115 (1981).
16. Levitt, D. G. & Levitt, M. D. Human serum albumin homeostasis: a new look at the roles of synthesis, catabolism, renal and gastrointestinal excretion, and the clinical value of serum albumin measurements. *Int. J. Gen. Med.* **9**, 229–255 (2016).
17. Kontoyiannis, D. P. et al. Zygomycosis in a tertiary-care cancer center in the era of *Aspergillus*-active antifungal therapy: a case-control observational study of 27 recent cases. *J. Infect. Dis.* **191**, 1350–1360 (2005).
18. Lanternier, F. et al. Prospective pilot study of high-dose (10 mg/kg/day) liposomal amphotericin B (L-AMB) for the initial treatment of mucormycosis. *J. Antimicrob. Chemother.* **70**, 3116–3123 (2015).
19. Jones, D. T. et al. Albumin activates the AKT signaling pathway and protects B-chronic lymphocytic leukemia cells from chlorambucil- and radiation-induced apoptosis. *Blood* **101**, 3174–3180 (2003).
20. Artis, W. M., Fountain, J. A., Delcher, H. K. & Jones, H. E. A mechanism of susceptibility to mucormycosis in diabetic ketoacidosis: transferrin and iron availability. *Diabetes* **31**, 1109–1114 (1982).
21. Ashraf, S. et al. Unraveling the versatility of human serum albumin—a comprehensive review of its biological significance and therapeutic potential. *Curr. Res. Struct. Biol.* **6**, 100114 (2023).
22. van der Vusse, G. J. Albumin as fatty acid transporter. *Drug Metab. Pharmacokinet.* **24**, 300–307 (2009).
23. Borreby, C., Lillebæk, E. M. S. & Kallipolitis, B. H. Anti-infective activities of long-chain fatty acids against foodborne pathogens. *FEMS Microbiol. Rev.* **47**, fuad037 (2023).
24. Abdelmagid, S. A. et al. Comprehensive profiling of plasma fatty acid concentrations in young healthy *Canadian adults*. *PLoS ONE* **10**, e0116195 (2015).
25. Chen, R. F. Removal of fatty acids from serum albumin by charcoal treatment. *J. Biol. Chem.* **242**, 173–181 (1967).
26. Augé, N., Santanam, N., Mori, N., Keshava, C. & Parthasarathy, S. Uptake of 13-hydroperoxylinoleic acid by cultured cells. *Arterioscler. Thromb. Vasc. Biol.* **19**, 925–931 (1999).
27. Pap, E. H. et al. Ratio-fluorescence microscopy of lipid oxidation in living cells using C11-BODIPY(581/591). *FEBS Lett.* **453**, 278–282 (1999).
28. Kimura, K., Yamaoka, M. & Kamisaka, Y. Rapid estimation of lipids in oleaginous fungi and yeasts using Nile red fluorescence. *J. Microbiol. Methods* **56**, 331–338 (2004).
29. Blache, D. et al. Glycated albumin with loss of fatty acid binding capacity contributes to enhanced arachidonate oxygenation and platelet hyperactivity: relevance in patients with type 2 diabetes. *Diabetes* **64**, 960–972 (2015).
30. Liu, J., Xu, Y., Stoleru, D. & Salic, A. Imaging protein synthesis in cells and tissues with an alkyne analog of puromycin. *Proc. Natl Acad. Sci. USA* **109**, 413–418 (2012).
31. Low, B. E. & Wiles, M. V. A humanized mouse model to study human albumin and albumin conjugates pharmacokinetics. *Methods Mol. Biol.* **1438**, 115–122 (2016).
32. Abdollahi, A., Dowden, B. N., Buhman, K. K., Zembroski, A. S. & Henderson, G. C. Albumin knockout mice exhibit reduced plasma free fatty acid concentration and enhanced insulin sensitivity. *Physiol. Rep.* **10**, e15161 (2022).
33. Roden, M. M. et al. Epidemiology and outcome of zygomycosis: a review of 929 reported cases. *Clin. Infect. Dis.* **41**, 634–653 (2005).
34. Zhang, J. et al. Risk factors for disease severity, unimprovement, and mortality in COVID-19 patients in Wuhan, China. *Clin. Microbiol. Infect.* **26**, 767–772 (2020).
35. Dos Santos, P. T., Thomasen, R. S. S., Green, M. S., Færgeman, N. J. & Kallipolitis, B. H. Free fatty acids interfere with the DNA binding activity of the virulence regulator PrfA of *Listeria monocytogenes*. *J. Bacteriol.* **202**, e00156-20 (2020).
36. Casillas-Vargas, G. et al. Antibacterial fatty acids: an update of possible mechanisms of action and implications in the development of the next-generation of antibacterial agents. *Prog. Lipid Res.* **82**, 101093 (2021).
37. Coonrod, J. D., Lester, R. L. & Hsu, L. C. Characterization of the extracellular bactericidal factors of rat alveolar lining material. *J. Clin. Invest.* **74**, 1269–1279 (1984).
38. Coonrod, J. D. & Yoneda, K. Detection and partial characterization of antibacterial factor(s) in alveolar lining material of rats. *J. Clin. Invest.* **71**, 129–141 (1983).
39. Kenny, J. G. et al. The *Staphylococcus aureus* response to unsaturated long chain free fatty acids: survival mechanisms and virulence implications. *PLoS ONE* **4**, e4344 (2009).
40. Egesten, A., Frick, I. M., Mörgelin, M., Olin, A. I. & Björck, L. Binding of albumin promotes bacterial survival at the epithelial surface. *J. Biol. Chem.* **286**, 2469–2476 (2011).
41. Hitzler, S. U. J. et al. Host albumin redirects *Candida albicans* metabolism to engage an alternative pathogenicity pathway. *Nat. Commun.* **16**, 6447 (2025).
42. Roche, M., Rondeau, P., Singh, N. R., Tarnus, E. & Bourdon, E. The antioxidant properties of serum albumin. *FEBS Lett.* **582**, 1783–1787 (2008).
43. Zhang, L., Wu, T. & Jia, H. Invasive pulmonary aspergillosis in patients with lung cancer: risk factors for in-hospital mortality and predictors of clinical outcomes. *J. Mycol. Med.* **35**, 101560 (2025).
44. Santos, A. et al. Hypoalbuminemia is a risk factor for invasive fungal infections and poor outcomes in infected kidney transplant recipients. *Clin. Transplant.* **37**, e15052 (2023).
45. Gremese, E. et al. Serum albumin levels: a biomarker to be repurposed in different disease settings in clinical practice. *J. Clin. Med.* **12**, 6017 (2023).
46. Leek, L. V. M. et al. Multi-omic analysis identifies hypoalbuminemia as independent biomarker of poor outcome upon PD-1 blockade in metastatic melanoma. *Sci. Rep.* **14**, 11244 (2024).
47. Baker, M. E. Albumin, steroid hormones and the origin of vertebrates. *J. Endocrinol.* **175**, 121–127 (2002).

[1]School of Medicine, University of Crete, Voutes, Heraklion, Greece. [2]Institute of Molecular Biology and Biotechnology, Foundation for Research and Technology, Heraklion, Greece. [3]Research Institute for Medical and Health Sciences, University of Sharjah, Sharjah, United Arab Emirates. [4]Centro de Metabolómica y Bioanálisis (CEMBIO), Facultad de Farmacia, Universidad San Pablo-CEU, CEU Universities, Urbanización Montepríncipe, Madrid, Spain. [5]Department of Pulmonary Medicine, Postgraduate Institute of Medical Education and Research (PGIMER), Chandigarh, India. [6]Department of Pharmacy, National and Kapodistrian University of Athens, Athens, Greece. [7]Division of Infectious Diseases, The Lundquist Institute for Biomedical Innovation, Harbor-University of California at Los Angeles (UCLA) Medical Center, Torrance, CA, USA. [8]Department of Hematology, University Hospitals Leuven, Leuven, Belgium. [9]Department of Infectious Diseases, Infection Control and Employee Health, University of Texas MD Anderson Cancer Center, Houston, TX, USA. [10]School of Medicine, National and Kapodistrian University of Athens, Athens, Greece. [11]Departamento de Genética y Microbiología, Facultad de Biología, Universidad de Murcia, Murcia, Spain. [12]Life and Health Sciences Research Institute (ICVS), School of Medicine, University of Minho, Braga, Portugal. [13]ICVS/3B's—PT Government Associate Laboratory, Guimarães/Braga, Portugal. [14]Institute for Hygiene and Microbiology, University of Würzburg, Würzburg, Germany. [15]Leibniz Institute for Natural Product Research and Infection Biology—Hans-Knoell-Institute, Jena, Germany. [16]Department of Medical Microbiology, Postgraduate Institute of Medical Education and Research (PGIMER), Chandigarh, India. [17]Unit of Clinical Research, AP-HP, University Necker Hospital, Paris, France. [18]Pharmacologie et Évaluations des Thérapeutiques Chez l'Enfant et la Femme Enceinte, Inserm, Université Paris Cité Inserm, Paris, France. [19]Service de Maladies Infectieuses et Tropicales, Hôpital Universitaire Necker-Enfants Malades, Assistance Publique-Hôpitaux de Paris, Université Paris Cite, Paris, France. [20]Department of Microbiology and Immunology, University of Maryland School of Medicine, Baltimore, MD, USA. [21]College of Pharmacy, University of Sharjah, Sharjah, United Arab Emirates. [22]David Geffen School of Medicine at UCLA, Los Angeles, CA, USA. [23]These authors contributed equally: Antonis Pikoulas, Ioannis Morianos, Vassilis Nidris. [24]Deceased: Kyriakos Petratos. ✉e-mail: hamilos@imbb.forth.gr

Methods

Microorganisms and culture conditions

R. delemar (99-880)[9], *R. arrhizus* (557969)[48] and *Cunninghamella bertholletiae* (506313)[48] have been previously described. *Mucor circinelloides* (JMRC:NRZ:0774), *Rhizomucor pusillus* (JMRC:NRZ:0496), *Rhizopus microsporus* (JMRC:NRZ:0680), *A. fumigatus* (ATCC, 46645), *Aspergillus flavus* (JMRC:NRZ:0756), *Aspergillus terreus* (JMRC:NRZ:0442), *C. albicans* (JMRC:NRZ:1000), *C. glabrata* (JMRC:NRZ:1006), *C. albicans* SC5314 and *Fusarium proliferatum* (JMRC:NRZ:0657) were obtained from the Leibniz Institute for Natural Product Research and Infection Biology, Hans Knöll Institute. All Mucorales isolates were cultured on potato dextrose agar (Becton Dickinson) plates for 7 days at 37 °C. *R. delemar* M16 is a previously described *pyrF*-null mutant derived from *R. delemar* 99-880 that is unable to synthetize uracil[49]. *R. delemar* transformed with RNAi targeting mucoricin expression and *R. delemar* transformed with empty plasmid (control) were derived from strain M16, as previously described[9]. For the experiments involving these RNAi strains, a synthetic medium containing yeast nitrogen base (YNB, BD) supplemented with a complete supplemental mixture without uracil (CSM−URA, MP Biochemicals) (that is, YNB + CSM−URA) was used.

All of the bacterial isolates used (*Escherichia coli, Pseudomonas aeruginosa, Klebsiella pneumoniae* and *Staphylococcus aureus*) were clinical isolates obtained from the University Hospital of Heraklion, Crete. All bacteria were streaked onto plates containing LB agar plates from a freshly prepared frozen glycerol stock. After growth on LB agar plates, single colonies were used to inoculate overnight cultures of LB (50 ml at 37 °C). The next day, a volume of 1 ml of each of these cultures was diluted 1:10 to a final volume of 10 ml in LB medium and incubated in conical flasks for 2 h, at 37 °C, with constant shaking, to reach mid-log phase of growth. A volume of 200 µl was taken from each culture and the optical density was measured at 600 nm (OD_{600}). The desired volume from each culture was used and centrifuged at 2,000 rpm for 2–3 min. Bacteria pellets were washed three times with LB medium. Bacteria pellets were diluted in RPMI medium or RPMI plus 4.5 g dl^{-1} of albumin to the desired OD_{600} of 0.2. A volume of 200 µl from each test condition was transferred to a flat-bottom 96-well plate. The plates were incubated at 37 °C, with constant shaking. At regular time intervals (45 min), 10 µl from each culture condition was diluted in RPMI medium to a final volume of 100 µl and the OD_{600} was measured spectrophotometrically. The mean value of triplicate measurements of bacterial growth in regular medium at $t = 340$ min was defined as 100% growth.

For filamentous fungi, the effect of albumin on fungal growth was assessed by counting spore germination rates in RPMI medium compared with RPMI supplemented with 4.5 g dl^{-1} albumin at 6 h using light microscopy. At least 300 spores were counted per condition in biological triplicates. For the effect of human IgG (i.v. human IgG, Gaminex, 100 mg ml^{-1}, Grifols) fungal spores were incubated in medium containing increasing concentrations of human IgG (from 1.5 g dl^{-1} to 4.5 g dl^{-1}). At 6 h, spores were assessed by light microscopy and photos were taken.

For *Candida* isolates, the impact of albumin on growth was evaluated spectrophotometrically. *C. albicans* strain SC5314 and *Candida glabrata* (JMRC:NRZ:1006) were streaked from freshly prepared glycerol stocks onto Sabouraud dextrose agar plates and incubated overnight at 37 °C. Single colonies were used to inoculate Sabouraud dextrose broth (50 ml) and liquid cultures were grown overnight at 37 °C with agitation at 150 rpm. The OD_{600} of the overnight cultures was determined, and aliquots were diluted with phosphate-buffered saline (PBS) to an OD_{600} of 0.1. Cells were collected by centrifugation at 2,000 rpm for 10 min, washed three times with PBS, counted and resuspended in either RPMI medium alone or RPMI supplemented with 4.5 g dl^{-1} albumin to an OD_{600} of 0.1. For each condition, 200 µl of the cell suspension was transferred into wells of a flat-bottom 96-well plate and incubated at 37 °C with continuous shaking. After 8 h, 10 µl from each well was diluted in RPMI to a final volume of 100 µl, and the OD_{600} was measured spectrophotometrically. Growth in standard RPMI medium was assessed in triplicate, and the mean OD_{600} value at 8 h was defined as 100% growth for normalization.

Human albumin depletion and purification

Albumin was depleted from human serum using an Albumin Depletion Kit (Abcam) according to the manufacturer's instructions with a modification in the rehydration step of Cibacron Blue 3G-A beads, which was performed using albumin-free serum filtrate (generated through serum filtration using Amicon 50 kDa molecular weight cut-off (MWCO) ultracentrifugal filters; Merck).

For HSA purification, Blue Sepharose 6 Fast Flow (GE Healthcare) was first rehydrated with an albumin-free serum filtrate, incubated with fresh human serum (3 ml) at 4 °C overnight with rotation and then packed back in a column. The first volume (3 ml) of the flow-through contained albumin-depleted human serum. The column was subsequently washed with 7 ml of wash buffer (20 mM Na_2HPO_4, 20 mM NaH_2PO_4, pH 8). Albumin was isolated from the column in six consecutive elutions using 7 ml of elution buffer (2 M NaCl, 20 mM Na_2HPO_4, pH 8) each time. Elution fractions 2–6 were pooled and further processed for in vitro experiments.

Owing to the increased amount of NaCl in the eluted fractions, dialysis was performed using a CelluSep T2 membrane (Orange Scientific, Cellusep T2 Tubings, 6,000–8,000 MWCO), which was embedded in the appropriate buffer (20 mM Na_2HPO_4, 20 mM NaH_2PO_4, pH 8) for 4 h at 4 °C to achieve a physiologically relevant NaCl concentration (150 mM). Elutions were then condensed using Amicon 3 kDa MWCO ultracentrifugal filters (Merck), to a final volume of 2 ml and filter-sterilized through 0.22 µm Spin-X centrifuge tube filters (Costar). The flow-through generated during the condensation procedure was pooled, measured for any remnants of albumin (no traces of albumin were found) and also filter-sterilized using the same 0.22-µm filters.

Chemical modifications of albumin

Highly oxidized albumin was prepared by the incorporation of cysteine into reduced albumin[50]. BSA was treated with a 50-fold molar excess of L-cysteine/cystine by mixing 80 ml of 0.06 mM BSA with 72 ml of 3 mM cysteine and 8 ml of 3 mM cystine. All of the solutions were diluted in 0.1 M sodium carbonate and hydrogen carbonate buffer (pH 10) and, after incubation at 37 °C for 48 h, the resulting mixture was lyophilized. Next, the residue was dissolved in PBS and purified from low-molecular-mass components (excess cysteine/cystine) by filtration through an Ultrafree-3000 Da membrane (Millipore) at 4 °C. Purified, highly oxidized albumin was lyophilized and stored at room temperature. Glycosylated albumin was prepared by diluting albumin in PBS containing 5 mM glucose[51]. The solution was incubated for 72 h under an atmosphere of 95% O_2, and 5% CO_2 to maintain the pH at 7.3–7.4. The mixture was then lyophilized, followed by solubilization in PBS and purification through ultrafiltration with an Ultrafree-3000 Da membrane. Purified, glycosylated albumin was lyophilized and stored at room temperature. The control solutions were prepared in PBS and subjected to the same lyophilization and filtration processes to increase the reliability of the results. The dried, equal-weight samples were derivatized with 20 µl of 20 mg ml^{-1} methoxy amine/pyridine and 50 µl of hexane. The mixture was vortexed and kept at 37 °C for 1.5 h, with vortexing every 30 min. Then, 90 µl (*N*-trimethylsilyl-*N*-methyl trifluoro-acetamide and trimethyl-chlorosilane (MSTFA + 1% TMS) were added and the samples were vortexed for 30 s and incubated at 37 °C for 1 h. The obtained solution was filtered through 0.45-µm syringe filters (nylon syringe filter, Membrane Solutions) and subjected to GC–MS/MS in multiple reaction monitoring (MRM) mode analysis according to previously published methods[52,53]. The obtained metabolites were imported into MetaboAnalyst (v.5.0; https://www.metaboanalyst.ca/home.xhtml). Hierarchical cluster analysis and partial

least squares-discriminant analysis were then performed according to previous methods[54].

The removal of FFAs from albumin (BSA and HSA isolated from donors) was performed with the use of activated charcoal, as previously described with some modifications[25]. Next, activated charcoal and albumin were mixed at a ratio of 1:2 for 1 h at 4 °C. The excess of activated charcoal was removed by ultracentrifugation at 20,200*g* for 30 min at 4 °C.

Loading of albumin with FFAs was performed as previously described[55,56] with some modifications. In brief, 4.5 g dl^{-1} charcoal-treated albumin (diluted in RPMI medium) and 80 mM FFAs (diluted in ethanol) were heated at 55 °C for 30 min and 5 min, respectively. Then, FFAs and albumin were gently mixed at a ratio of 8:1. The FFA–albumin mixture was thoroughly mixed by vortexing and incubated at 37 °C for 1 h. Effective conjugation of FFAs to albumin resulted in a clear solution.

Extraction and quantification of caprylic acid in glycosylated and non-glycosylated BSA

Quantification of caprylic acid in glycosylated and non-glycosylated BSA was conducted by extracting caprylic acid using chloroform/methanol solvent (2:1, v/v)[57]. This was followed by centrifugation at 3,500 rpm to separate the organic layer, which was filtered through anhydrous sodium sulphate and then dried using a rotary evaporator (Büchi). The dried residue was subsequently derivatized and analysed using GC–MS/MS in MRM mode against standard caprylic acid (*m*/*z* 201.10, 117.10 and 75.00).

Fluorescence displacement assay of caprylic acid binding with glycosylated and non-glycosylated BSA

The fatty-acid binding affinity of glycosylated and non-glycosylated BSA was assessed using the 1-anilino-8-naphthalene sulfonic acid (ANS) fluorescence displacement assay according to a previously established protocol[58]. In brief, BSA solutions (2.5 μg in 100 μl PBS) were added into black 96-well flat-bottom microplates (Nunc Microwell Plates), followed by the addition of 50 μl ANS in PBS to a final concentration of (0, 1.25, 2.5, 5 and 10 μM) with incubation at room temperature in dark for 15 min. For the displacement assay, caprylic acid was added at increasing concentrations (0–10 μM) to the ANS–BSA complexes. A control without caprylic acid was included to assess the initial fluorescence. The mixtures were incubated at room temperature in the dark for an additional 15 min. Measurements were performed using a microplate reader (Synergy H1, Biotek) with excitation and emission wavelengths set at 360 nm and 460 nm, respectively. Fluorescence quenching, indicative of ANS displacement by caprylic acid, was recorded as the percentage change in fluorescence intensity (Δ*F*%) using the formula: $\%\Delta F \text{ quenching} = [(F_0 - F_1)/F_0] \times 100$, where F_0 is the fluorescence in the absence of caprylic acid and F_1 is the fluorescence at each tested concentration of caprylic acid.

In vitro assessment of the inhibitory activity of albumin and human serum

Fungal conidia (spores) were collected by gentle shaking in the presence of sterile 0.1% Tween-20 in PBS, washed twice with PBS, filtered through a 40-μm-pore-size cell strainer (Falcon) to separate conidia from contaminating mycelium, counted using a haemocytometer and suspended at a concentration of 10^8 spores per ml. To achieve synchronized swelling of *Rhizopus* conidia, 1×10^6 per ml dormant conidia were incubated for 4–6 h at 28 °C in a six-well plate in RPMI-MOPS (pH 7.0) supplemented with 2% glucose with or without 4.5 g dl^{-1} BSA or other sources of albumin. To study the minimal growth requirements of *R. delemar*, a minimal-growth-requirements medium was used[59] based on HBSS supplemented with 0.05% (w/v) $MgSO_4 \cdot 7H_2O$, 0.1% (w/v) glucose and 0.1% (w/v) NH_4Cl (minimal medium). For fluorescence labelling, the spores were stained with 20 μg ml^{-1} Fluorescent Brightener 28 (Calcofluor White; CFW, Sigma-Aldrich) in 0.1 M $NaHCO_3$ pH 8.3 at room temperature in the dark for 1 h, with constant rotation.

In another set of experiments, *R. delemar* spores were incubated at 37 °C in RPMI-MOPS without phenol red adjusted to pH 7, for 2 h to start swelling. Then, 3.6 g dl^{-1} BSA and 900 μg ml^{-1} FITC-albumin (Sigma-Aldrich) were added to the medium and the spores were cultured in a 96-well μ-Plate (Ibidi) at 37 °C. After 5 h of culture, *R. delemar* live spores were collected, washed twice with PBS and then stained with 100 μg ml^{-1} CFW in 0.1 M $NaHCO_3$ pH 8.3 at room temperature in the dark for 1 h, with constant rotation. Fungal cells were then imaged with a spinning-disk confocal microscope (Dragonfly 200, Andor).

To assess the inhibitory activity of human serum, 1×10^4 fungal spores were incubated in flat-bottom 96-well plates containing 100 μl of serum from healthy individuals or patients at 37 °C and 5% CO_2 for 5–6 h. At least three different fields of each well (a total of >100 germinating spores) were imaged under an inverted microscope (Olympus) and the length of the germinating conidia was measured using ImageJ[60]. In certain experiments, time-lapse videos of fungal growth were acquired using an Operetta high screening content system (Perkin Elmer) at room temperature with 5% CO_2. Photographs of each well were automatically taken approximately every 30 min for 18 timepoints and analysed using Harmony v.4.1 software (Perkin Elmer).

The inhibition of fungal growth was additionally quantitated via an XTT metabolic activity assay (Biotium). A solution of XTT tetrazolium salt (0.25 mg ml^{-1}) and menadione (25 μM) was freshly prepared in PBS and added to the cell culture. Fungal spores were further incubated at 37 °C for another 1 h (ref. 61). Fungal-spore-free culture supernatants were collected, and their absorbances at 450 nm (OD_{450}) and 620 nm (OD_{620}) were measured using a microplate photometer (Multiscan, Thermo Fisher Scientific). Growth inhibition was calculated according to the following formula:

$$\text{Growth inhibition}(\%) = 100 \times \frac{(OD_{450} - OD_{620})_{\text{control cells}} - (OD_{450} - OD_{620})_{\text{treated cells}}}{(OD_{450} - OD_{620})_{\text{control cells}}}$$

In vitro studies on the antimicrobial activity of FFAs

FFA stock solutions were initially dissolved in absolute ethanol to a final concentration of 80–1,000 mM and incubated at 95 °C for 5 min. 2× MOPS-RPMI medium was also heated at 95 °C for 30 min and serial dilutions of FFAs were made by slowly adding the desired volume of preheated FFAs into the medium. The final concentration of ethanol used under culture conditions was 5% to ensure optimal dilution of FFAs; we confirmed that 5% ethanol had no significant inhibitory effect on Mucorales growth. Fungal spores were incubated in FFA-containing MOPS-RPMI medium at 37 °C for 16–18 h and fungal germination was measured as previously described[13].

Lipid extraction

Lipids were extracted using a $CHCl_3$:CH_3OH (2:1) solution according to a previously published method[62], dried with anhydrous sodium sulfate, subjected to residual evaporation via a rotatory evaporator (Buchi) under an inert stream of nitrogen and then stored at −20 °C (ref. 63). The residue obtained was equally divided into two parts; one for the oxidation reaction and the other left under inert conditions to avoid auto-oxidation.

Microwave-assisted oxidation of FFAs

FFAs and BSA-bound FFAs were subjected to oxidation through an irradiation microwave reactor according to modified previously published methods[64]. The samples were dissolved in 0.2 mM H_2O_2 in methanol to a final volume of 10 ml. The oxidization reaction was performed in a sealed vial on a synergy microwave synthesizer (CEM) for 20 min at an operating temperature of 100 °C and a pressure of 200 psi. The reaction

mixture was extracted with $CHCl_3$, dried with anhydrous sodium sulfate, subjected to residual evaporation through a rotatory evaporator (Buchi) and stored at −20 °C.

Open-air-assisted oxidation of FFAs

FFAs (OA), human or mouse plasma lipid extracts were diluted in absolute ethanol and exposed to open air inside a laminar flow hood as previously described[65]. After 4 days, ethanol was evaporated, and the precipitates of the oxidized FFAs were rediluted to their initial volume in 0.01 M Tris-HCl pH 7.5 (human and mouse plasma lipids) or in absolute ethanol to a final concentration of 80 mM (OA) and stored at −20 °C.

Cell damage assay for the assessment of toxin neutralizing activity of albumin

Human alveolar epithelial cells (A549 cells) were obtained from a 58-year-old male Caucasian patient with carcinoma and procured from American Type Culture Collection (ATCC). The cells were propagated in F-12K Medium developed for lung A549 epithelial cells. The damage of A549 epithelial cells was quantified using a ^{51}Cr-release assay[9,66]. In brief, confluent cells grown in 24-well tissue culture plates were incubated with 1 µCi per well $Na_2{}^{51}CrO_4$ (ICN) in F12K-medium for 16 h. On the day of the experiment, the medium was aspirated, and cells were washed twice with pre-warmed Hanks' balanced salt solution (HBSS, ScienCell). Cells treated with mucoricin with or without the addition of albumin (free of FFAs BSA at a final concentration of 4.5 g dl^{-1}) were suspended in 1 ml of F12K-medium supplemented with glutamine and incubated at 37 °C in a 5% CO_2 incubator. Spontaneous ^{51}Cr release was determined by incubating the untreated cells in the same volume of the culture medium supplemented with glutamine. At different timepoints, and after data were corrected for variations in the amount of tracer incorporated in each well, the percentage of specific cell release of ^{51}Cr was calculated as follows: [(experimental release) − (spontaneous release)]/[1 − (spontaneous release)][66]. Each experimental condition was tested at least in triplicate, and the experiment was repeated at least twice.

Ethics statement on human clinical studies

All research involving human participants was conducted in accordance with relevant ethical regulations and approved by the ethics committees of the respective participating institutions. All patients or their legal representative provided written informed consent for the collection of clinical samples analysed in this study, in accordance with the Declaration of Helsinki.

The medical records of contemporaneous patients who had been admitted at the Leukemia Department of the MD Anderson Cancer Center were retrospectively reviewed. Standardized EORTC/MSG criteria were applied for diagnosis of pulmonary mucormycosis and pulmonary aspergillosis[67]. Clinical information of matched control patients for the underlying disease who developed bacterial (*Legionella*) pneumonia were also reviewed. Albumin levels were retrieved from the medical records of all of the patients on the day of hospital admission. Information on demographics, underlying disease and risk factors for mucormycosis were collected. The study was approved by the Institutional Review Board (IRB) of The University of Texas MD Anderson Cancer Center (MDACC; protocol PA14-0802).

The medical records of consecutive patients admitted to the Department of Pulmonary Medicine, Department of Medical Microbiology, Institute of Medical Education and Research (PGIMER), Sector-12, Chandigarh, 160012, India over the past 8 years (2016–2023) with a diagnosis of pulmonary mucormycosis were retrospectively evaluated. The study was approved by the Institutional Ethics Committee (IEC; Intramural; INT) of the PGIMER (IEC/INT, 2023/study-1564) and registered with the Biological Research Regulatory Approval Portal (BIORRAP, POS36452025). All procedures were conducted in accordance with institutional and national guidelines and regulations.

Serum samples were prospectively collected from healthy individuals, patients with cirrhosis and patients with haematological malignancies at the University Hospital of Heraklion, Crete, and the Therapeutics Clinic of the General Hospital of Athens "Alexandra". Demographics, clinical characteristics, serum albumin levels, total FFAs and oxidized FFA levels were measured in the sera of healthy individuals and patients. Approval for the collection of clinical information and blood samples from all individuals mentioned above was obtained from the Ethics Committee of the University of Heraklion, Crete, Greece (5159/2014, 10925/201 and 13-04-22/7970) and Therapeutics Clinic (122/18-2-2021).

For lipidomic and functional studies, serum samples from patients with mucormycosis or invasive pulmonary aspergillosis, and from matched control patients were obtained from patients with haematological malignancy admitted to the University Hospitals of Leuven, Belgium (IRB, S61797).

Vitamin quantification in culture medium using LC–MS

Samples were first filtered through 0.22-µm nylon syringe filters before undergoing LC–MS/MS analysis. The analysis was performed via an Elute UHPLC system linked to a Q-TOF mass spectrometer. Chromatography separation was performed on a Hamilton Intensity Solo C18 column, maintained at 35 °C. The sample mixture was 10 µl in a solvent system composed of 0.1% formic acid in deionized water (solvent A) and acetonitrile (solvent B). The elution gradient progressed from 1% to 99% solvent B over 20 min, with flow rates adjusted between 0.25 ml min^{-1} and 0.35 ml min^{-1}. Vitamin detection followed established methods by employing standards of cyanocobalamin (B12), folic acid (B9), riboflavin (B2), thiamine (B1), biotin (B7), Ca-panthenoate (B5), pyridoxine (B6), nicotinamide (B3), choline chloride and PABA, all sourced from Sigma-Aldrich. Stock solutions of 5 mM for vitamins B1, B3, B5, B6, B7, B9 and B12, and choline chloride were prepared in water, with riboflavin (B2) in DMSO. Internal standard solutions were made at 10 mM, and working solutions comprised 200 mM of all vitamins in water and 100 mM of internal standards. Calibration curves were prepared using 0.1% formic acid in water, spanning six serial dilutions from 0 to 100 mM, each including 2.5 mM internal standards. Samples and calibration solutions underwent identical processing involving liquid-liquid extraction and drying before analysis, ensuring precise quantification of vitamins with detection limits in the low µg l^{-1} range. Each sample was injected three times.

Analysis of trace elements in culture medium using ICP-MS

Inductive coupled plasma MS (ICP-MS-9800 Series) was used to detect trace metals in the samples. The samples were collected and digested with hydrochloric acid, to ensure complete dissolution. Microwave-assisted digestion was used for rapid and efficient sample preparation. The digested samples were then diluted with deionized water such that the concentration was within the measurable range of the ICP-MS instrument. Calibration standards with known concentrations of Na, K, Ca, Mg, Cu and Fe were prepared, and isotope-labelled internal standards were used to correct for matrix effects and signal fluctuations. The prepared samples were injected into the ICP-MS instrument through a nebulizer, which converts the liquid sample into an aerosol. The ionized elements emit light at characteristic wavelengths, which are detected and quantified by a mass spectrometer. The concentrations of trace elements in the samples were calculated by comparing the sample signals to the calibration curve.

Analysis of amino acids in culture medium

The samples were centrifuged at 12,000 rpm for 10 min and the supernatants were analysed using the Waters Acquity ultra-performance liquid chromatography (UPLC) H-Class-Xevo TQD system equipped with ESI. HPLC was performed using the Acquity BEH C18 column (1.7 µm, 2.1 mm × 150 mm). The binary mobile phase consisted of solvent A (100% methanol) and solvent B (0.2% formic acid). The column gradient

was as follows: 100% B for 10 min; 66.6% B for 0.5 min; returned to 100% B for 1 min; and maintained at 100% B for another 0.5 min. The flow rate was 0.2 ml min^{-1}, the injection volume was 10 µl and the column effluent was monitored by MS. The MS analysis was performed in MRM mode in positive-ionization mode. The MS parameters were as follows: the dwell time was 0.02 s, and nitrogen was used as a desolvating gas at a flow rate of 600 l h^{-1}. The ionization source conditions were as follows: desolvation temperature 350 °C; source temperature 150 °C; collision gas (argon) flow 0.1 ml min^{-1}; and capillary voltage 3.0 kV. The parameters of mass analyser were set as follows: the LM1 and HM1 resolutions were 15 and 15, respectively, as ion energy 1; the LM2 and HM2 resolutions were 15 and 15, respectively, and the ion energy was 2. The amino acids in the samples were identified on the basis of the mass-to-charge ratio.

The quantification of amino acids was conducted using a standard mix calibration curve, with the UPLC–MS/MS system controlled by Lynx software (v.4.1, SCN 882). Data analysis was performed via the TargetLynx program. Each sample, which contained a mixture of amino acids at specific concentrations, was injected three times to ensure accuracy. The amino acid standard solution (AAS18, Sigma-Aldrich) included 2.5 µmol ml^{-1} of various amino acids such as L-alanine, L-arginine and L-valine, with L-cystine at 1.25 µmol ml^{-1}. The samples were diluted in 0.1% formic acid in water for analysis. Using the MIDAS workflow, full scan linear ion trap MS/MS data confirmed the identity of the target analytes. MRM extracted ion chromatograms were used for all amino acids, especially at concentrations near their limits of detection, ensuring precise quantification and linearity. Limits of detection were accurately calculated for all amino acids, and their concentrations were measured.

Albumin ligand analysis and fractionation

BSA was added to minimal growth requirements medium to a final concentration of 4.5 g dl^{-1}, left at room temperature for 0.5–1 h and then filtered through Amicon 3 kDa MWCO ultracentrifugal filters (Merck) to remove albumin. BSA after filtration (15 ml) was subjected to fractionation through C-18 solid-phase extraction. After conditioning with 6 ml of methanol and 6 ml of ultrapure water, 15 ml of the sample was applied, giving fraction 1 (F1). Subsequently, with gradual elution (6 ml of 5% methanol), fraction 2 (F2) was obtained. Finally, fractions 3 (F3) and 4 (F4) were obtained using 6 ml of 50% methanol and 6 ml of pure methanol, respectively. During the entire process, the flow rate was held constant at approximately 3 ml min^{-1}. The solvents and reagents used were of LC-MS grade (Merck).

For fraction component identification through GC-MS analysis, the obtained fractions (1–4) were derivatized with methyl-chloroformate (Sigma-Aldrich). Specifically, 300 µl of every fraction was mixed with 80 µl of pyridine, 200 µl of methanol and 50 µl of methyl-chloroformate, vortexed for 30 s and incubated for 6 min at room temperature. After incubation, 1 ml of hexane was added to each reaction mixture and extracted via the liquid-liquid extraction technique. Finally, the hexane phase was subjected to GC-MS analysis.

Fractions F1–F4 were analysed through gas chromatography coupled with a single quadrupole MS (GC-MS) analyser. GC-MS analysis was performed with an Agilent gas chromatography instrument (model 8860) system coupled to a mass spectrometer (model 5970) using an electron ionization (EI) source.

The samples were qualitatively analysed and caprylic acid (or octanoic acid) was identified (NIST 14.0 EI spectral library) as the main component of F2. Furthermore, the caprylic acid structure was verified using a reference standard (Sigma-Aldrich), and its concentration was quantitatively determined in all four fractions, following the same derivatization protocol and a standard solution calibration curve. The entire analysis was conducted in duplicate. F2 was the richest in caprylic acid, with an average concentration of 194.1 µg ml^{-1}, followed by F3, with a much lower concentration of 15.2 µg ml^{-1}. In F1 and F4, only traces of caprylic acid were detected.

F2 was also analysed using HRMS without any derivatization steps to verify the structure of caprylic acid. Specifically, an UPLC system coupled with a HRMS analyser, especially a triple-TOF 5600+ (AB SCIEX) system, was used in negative ESI mode. LC analysis was performed on the ACQUITY H-Class UPLC system (Waters) equipped with a binary solvent manager and an FTN sample manager. A volume of 10 µl of F2 was injected into the system and separated by a linear gradient containing water and acetonitrile (mobile phases A and B, respectively, 5–100%), with the aqueous phase containing 0.1% formic acid. The solvents were of LC-MS grade and purchased from Merck. The analysis was performed with a Fortis Speedcore Biphenyl reversed-phase chromatography column (2.6 µm, 2.1 mm × 100 mm). The Triple-TOF platform was equipped with a DuoSpray ion source. The acquisition mode used was data dependent, covering a mass range of 80–500 *m/z*. Specifically, the tripleTOF parameters for acquisition were as follows: source temperature of 450 °C, source voltage of −4,500 V, exhaust gas pressure of 50 psi and curtain gas pressure of 35 psi. The caprylic acid structure was verified at *m/z* 143.1079 [M-H]- a, with a mass error of 1.1 ppm and degree of unsaturation (rings and double bond equivalents) of 1 (Extended Data Fig. 4).

FFA extraction from human plasma

FFAs were extracted from 100 µl of previously thawed plasma by the addition of 300 µl of cold methanol/ethanol (1:1) (Thermo Fisher Scientific). C17-Sphinganine was added as an internal standard. The samples were vortexed for 1 min, incubated on ice for 5 min and centrifuged at 16,100*g* for 20 min at 4 °C, after which 100 µl of the supernatant was transferred into LC–MS vials for analysis.

FFA extraction from the plasma of albumin-KO mice

FFAs were extracted from 100 µl of previously thawed plasma by the addition of 300 µl of cold methanol (Thermo Fisher Scientific). Next, 10 µl of 2 µM 9(S)-HODE-d4 solution (Cayman Chemical) was added as an internal standard. The samples were vortexed for 2 min and then centrifuged at 16,100*g* for 10 min at 4 °C, after which 100 µl of the supernatant was transferred into LC-MS vials for analysis.

Non-targeted analysis by LC–MS for FFAs

LC–MS analysis was performed on a UHPLC system 1290 Infinity II (Agilent Technologies) coupled with a 6546 QTOF MS detector in negative ESI mode. For separation, a volume of 1 µl was injected onto a Zorbax Rapid Resolution High Definition Extend-C18 column (Agilent Technologies, 2.1 × 50 mm, 1.8 µm) thermostated at 60 °C. The flow rate was 0.6 ml min^{-1}, with a mobile phase composed of ultrapure Milli-Q water with 0.1% formic acid for A and acetonitrile with 0.1% formic acid for B. The chromatography gradient started from 5% B for the first min and increased to 80% B in 6.0 min, then to 100% by 11.0 min, and the starting conditions were returned to 1.0 min, allowing re-equilibration until 15.0 min. Data were collected in negative ESI ionization mode and operated in the range of *m/z* 100–600 and *m/z* 40–600 for MS/MS analysis using iterative Agilent mode. The nozzle voltage was set to 1,000 V, and the capillary voltage was −4,000 V with a scan rate of 1.2 scans per s. The drying gas was heated to 250 °C at a rate of 12 l min^{-1} and a pressure of 52.0 psi. Additional heating was applied using sheath-heated gas up to 370 °C with a flow rate of 11 l min^{-1} to improve ionization. For internal mass correction during data acquisition, one reference mass was infused continuously into the system throughout the whole analysis: *m/z* 112.9856 (proton-abstracted TFA anion). An external calibration with FA 18:0 was used for semi-quantification of fatty acid species. Calibration curve samples were prepared at different concentrations (1.0, 2.5, 5.0, 10.0, 13.0, 17.0 and 20.0 ppm), and 9(S)-HODE-d4 was included as an internal standard at the same concentration as the serum samples. The raw data collected by LC-MS were reprocessed with MassHunter Profinder software v.B.10.02. Calibration curves were built using normalized values of FA 18:0 by d4-9-HODE versus concentration in

ppm. The results are expressed as the concentration in mM of the corresponding fatty acid in the serum. Detailed methods for identification of serum oxylipins and the standards used for the analysis of FFAs are provided in the Supplementary Methods.

RNA isolation from *R. delemar* cells

At the indicated timepoints of incubation in medium with or without albumin (0 h, 3 h and 6 h), the *R. delemar* cells were removed by scraping, centrifuged at 400*g* and lysed with 450 µl of RLT buffer + β-mercaptoethanol using the RNeasy Plant Mini Kit (Qiagen). Each sample was subsequently sonicated using a sonication probe on ice for 20 × 1 s (set 40). RNA was then isolated according to the manufacturer's instructions.

RNA-seq data generation and analysis

RNA-seq libraries (strand-specific, paired-end) were generated from total RNA by using a TruSeq RNA sample prep kit (Illumina). In total, 150 nucleotides of sequence were determined from both ends of each cDNA fragment using the HiSeq 4000 platform (Illumina). Sequencing reads were aligned to the reference genome (*R. delemar* 99-880) using STAR aligner (v.2.7.10)[68]. The reads that mapped to genomic features were calculated using the featureCounts program (v.2.0.3)[69]. Statistical analysis of differential gene expression was performed using the DEseq2 R-based package[70]. A gene was considered differentially expressed if the absolute log fold change was greater than or equal to 1 and the false-discovery rate value for differential expression was below 0.05. The RNA-seq analysis was performed in biological triplicate. RNA-seq data were generated by Maryland Genomics at the Institute for Genome Sciences, University of Maryland School of Medicine.

RNA-seq enrichment analysis

The GO enrichment analysis performed using the gene set enrichment analysis (GSEA)[71] method as previously implemented by the web-based application FungiFun3 (https://fungifun3.hki-jena.de/)[72]. The BlastKOALA automatic annotation server[73] was used for the functional annotation and the assignment of the KEGG orthologies. The pathway enrichment analysis performed using the generally applicable gene-set enrichment method[74] and functions of the gage R-based package. The genes of the selected KEGG pathways were identified using the KEGG PATHWAY database. R programming language was used for the visualization of the results. The heat maps were produced using the pheatmap package[75]. All of the *P* values were adjusted using the Benjamini–Hochberg method and adjusted $P < 0.05$ was considered to be statistically significant.

Animal studies

B6.Cg-Tg(FCGRT)32Dcr Alb^{em12Mvw} *Fcgrt*$^{tm1Dcr/MvwJ}$ mice, referred to as *Alb*$^{-/-}$ mice throughout (obtained from The Jackson Laboratory), and C57BL/6 mice were maintained in grouped cages in a high-efficiency air-filtered, environmentally controlled, virus-free facility (24 °C, 50–60% relative humidity, 12 h–12 h light–dark cycle) and fed a standard chow diet and water ad libitum.

Ethics statement on animal studies

All experiments were approved by the local Ethics Committee of the University of Crete Medical School, the FORTH Ethics Committee, and the Directorate of Agricultural and Veterinary Policy of the Region of Crete, in accordance with national and European Union legislation (animal protocols 17/07/2017-147075 and 22/03/2023-90477). All efforts were made to minimize the number of animals used and their suffering.

In vivo studies of fungal infection

For virulence studies, 8–12-week-old, age- and sex-matched mice were infected either through i.v. inoculation or through i.t. instillation of 1–5 × 10^6 spores of *R. delemar* or *A. fumigatus*, and their survival was monitored for 14–25 days. After infection, two mice from each group were euthanized for inoculum verification. For histopathological evaluation, lungs were collected at different timepoints: 0 h, 6 h and 1 day after infection. In a separate experiment, age- and sex-matched C57BL/6 mice were infected as above and then euthanized on day +1 after infection. Lungs were collected and processed to determine tissue fungal burden by qPCR. Approximately half of the lung tissue was snap frozen in ethanol/dry ice and stored at −80 °C until analysed[76]. In brief, lungs were homogenized in Whirl Pak bags (Thermo Fisher Scientific). Approximately 1.5 ml of the homogenate was transferred to sterile screw-cap lysing matrix tubes with 1.4-mm-diameter glass beads (MP Biomedicals). The homogenate containing mouse tissues and fungal hyphae was mechanically disrupted using Fastprep FP120 (Bio Thermo Electro Corporation) with three bursts of 30 s at speed 4 (with incubation on ice between bursts). The supernatant was collected from the secondary homogenate by centrifugation at 800*g* for 5 min at 4 °C. DNA was extracted from secondary homogenate with the DNeasy tissue kit (Qiagen) according to the manufacturer's instructions. DNA was recovered in 200 µl of elution buffer and stored at 20 °C until analysis by qPCR. Oligonucleotide amplification primers of the *R. oryzae* 18S rRNA gene (GenBank: AF113440) were designed with Primer Express software (v.1.5; Applied Biosystems) and synthesized commercially (Sigma-Aldrich). The sequences of these oligonucleotides are as follows: (i) sense amplification primer, 5′-GCGGATCGCATGGCC-3′; and (ii) antisense amplification primer, 5′-CCATGATAGGGCAGAAAATCG-3′. The qPCRs were performed as described previously[76]. Five-point standard curves were prepared by spiking uninfected lungs with known concentrations of *R. oryzae* sporangiospores, extracting total lung DNA, and then analysing *R. oryzae*-specific nucleic acid concentrations by qPCR. The standard curve created by spiking spores was used to calculate $\log_{10}$-transformed spore equivalents per gram of tissue.

For the establishment of immunosuppression/neutropenia, 8–12-week-old age- and sex-matched mice were administered three intraperitoneal injections of cyclophosphamide (Sigma-Aldrich, 150 mg per kg body weight on days −4 and −1, 100 mg per kg on day +3) and a subcutaneous injection of cortisone acetate (Sigma-Aldrich, 300 mg per kg on day −1), as previously described[77]. The mice were then infected i.t. with 1 × 10^6 spores of *R. delemar*. For the prophylactic model, 50 mg of FFA-free HSA was administered intraperitoneally on days −6, −4 and −2 prior to pulmonary infection with *R. delemar*. For the pre-emptive therapeutic model, 25 mg of FFA-free HSA was administered intraperitoneally daily for 6 consecutive days starting 6 h after pulmonary infection with *R. delemar*.

For the model of disseminated candidiasis, the *C. albicans* strain SC5314 was subcultured twice at 37 °C for 48 h on Sabouraud dextrose agar. After the second subculture, single *C. albicans* colonies were placed in liquid Sabouraud dextrose medium and grown for 16–18 h in a shaking incubator at 30 °C and 150 rpm. *Candida* blastoconidia were collected, centrifugated at 2,000 rpm for 10 min, washed three times in PBS, counted and reconstituted in PBS to a final concentration of 5 × 10^6 cells per ml. Then, 150 µl of *C. albicans* cells diluted in PBS (7.5 × 10^5) were used to i.v. infect 10–12-week-old, age- and sex-matched, wild-type C57BL/6 and *Alb*$^{-/-}$ mice, as previously described[78]. The viability of the inoculated *C. albicans* blastoconidia was assessed by performing serial dilutions in PBS and plating onto Sabouraud dextrose agar. Plated *C. albicans* cells were incubated at 37 °C overnight and the next day the number of colonies was counted and the inoculum validated.

Histopathology and immunohistochemistry/immunofluorescence studies

The mice were euthanized, and their lungs were excised and fixed with 10% formalin before being embedded in paraffin and cut into 5–7 µm sections. Lung tissue sections were deparaffinized in xylene and rehydrated through an ethanol gradient (100–70%). H&E or GMS (Sigma-Aldrich) staining was performed for histopathology and fungal

burden assessment, according to the manufacturer's instructions. For histological quantification of fungal burden[79], FFPE lung sections were stained with GMS to visualize fungal elements. In certain experiments, fungal conidia were counterstained with periodic acid-Schiff (PAS). Images were acquired from at least ten non-overlapping fields per section at ×10 magnification. Fungal hyphae were enumerated per high-power field in a blinded manner by an experienced pathologist.

For active caspase-3 immunostaining in the lung tissue, heat-induced antigen retrieval was performed to deparaffinize and rehydrate the lung sections through incubation in sodium citrate buffer (10 mM, 0.05% Tween-20, pH 6) for 40 min at 90–95 °C using a steamer (Philips). The tissue sections were allowed to cool for 30 min, washed three times in PBS and blocked endogenous peroxidase with 3% H_2O_2 for 10 min. The slides were then incubated in blocking solution (serum-free protein block, Dako) for 20 min to block nonspecific binding. The primary antibody was added to the slides at a 1:200 dilution and incubated overnight in a humidified chamber at 40 °C Detection was accomplished using an Envision Horseradish Peroxidase Kit (Dako). Immunostaining was revealed using 3,3′-diaminobenzidine (Dako). The slides were lightly counterstained with haematoxylin, progressively dehydrated through graded alcohols and xylene, and finally covered with a coverslip after mounting in DPX mounting medium. Slides were examined under an Olympus light microscope that was equipped with a ×40 objective.

For mucoricin immunostaining in the lung tissue, heat-induced antigen retrieval was performed to deparaffinize and rehydrate the lung sections through incubation in sodium citrate buffer (10 mM, 0.05% Tween-20, pH 6) for 40 min at 90–95 °C using a steamer (Philips). The tissue sections were allowed to cool for 30 min, washed three times in PBS and permeabilized in 0.2% gelatin/Triton X-100 0.25% for 15 min at room temperature, followed by blocking in 5% BSA/5% normal goat serum (NGS)/PBS for 1 h at room temperature. The tissue slices were subsequently incubated at 4 °C overnight with an anti-mucoricin antibody (2 mg ml^{-1}) in 1% BSA/1% NGS/PBS. The samples were washed three times with PBS then incubated with goat anti-rabbit CF488A or CF555 (1:500, Biotium) in the presence of 200 mg ml^{-1} CFW for 1 h at room temperature. The tissue sections were incubated for 10 min at room temperature with the nuclear dye TO-PRO-3 (1:2,000, Thermo Fisher Scientific), washed three times with PBS and quenched for autofluorescence by incubation in a solution of 10 mM $CuSO_4$/50 mM NH_4Cl.

For mucoricin and CotH3 immunostaining in *R. delemar*, spores were cultured at 30 °C in RPMI or RPMI supplemented with either 4.5 g dl^{-1} BSA, 4.5 g dl^{-1} BSA flow-through or 1 mM caprylic acid for 6-8 h until they swelled. The swollen spores were fixed in 4% paraformaldehyde for 10 min, followed by permeabilization in 0.1% Triton X-100 in PBS for 10 min at room temperature. The permeabilized spores were blocked with 5% NGS in PBS for 1 h at room temperature and subsequently incubated with the anti-mucoricin antibody (10 μg ml^{-1}) or anti-CotH3 antibody (100 μg ml^{-1})[10] for 2 h at room temperature. The spores were washed with Tris-buffered saline (0.01 M Tris HCl/0.15 M NaCl, pH 7.4) containing 0.05% Tween-20 and incubated with goat anti-rabbit CF488A (Biotium) diluted 1:500 in PBS for 1 h at room temperature.

Protein synthesis assessment in *R. delemar*

R. delemar spores were cultured in black 96-well cell culture plates with a #1.5 glass-like polymer cover slip bottom optimized for high resolution microscopy (P96-1.5P, IBL Baustoff+Labor) at a density of 1.5×10^5 per 200 μl per well. Fungal spores were cultured in RPMI/MOPS (pH 7) supplemented with 0.2% glucose with or without 4.5 g dl^{-1} BSA flow-through or 2 mM caprylic acid, at 37 °C and 5% CO_2. After 2 h (RPMI only) or 3 h (RPMI + BSA flow-through or RPMI + caprylic acid) of culture, media were replenished with OP-puro working solution prepared in the respective media of each treatment group, according to the recommendations of the Protein Synthesis Assay Kit protocol (Cayman Chemical). After 2 h of culture at 37 °C under 5% CO_2, *R. delemar* spores were fixed with the Cell-Based Assay Fixative, washed thrice with the cell-based assay wash buffer and incubated with 5 FAM-azide staining solution in the dark, at room temperature for 30 min. After three washes with cell-based assay wash buffer, *R. delemar* spores were preserved in 1× assay buffer and imaged directly with a spinning disk confocal microscope (Dragonfly 200, Andor), using the 488 nm/535 nm excitation/emission detection parameters.

Assessment of C12-BODIPY uptake by *R. delemar*

CFW-labelled *R. delemar* spores were cultured in RPMI/MOPS (pH 7) for 3 h at 37 °C. To assess whether *R. delemar* fungus uptakes lipids actively or passively, fungal spores were further cultured at 37 °C or 0 °C for 1 h, in RPMI/MOPS supplemented with 2 μM C12-BODIPY (Invitrogen). Active endocytosis events are inhibited at 0 °C, whereas passive diffusion events remain unaffected[80,81]. Subsequently, *R. delemar* spores were washed twice with ice-cold PBS and imaged in PBS using a spinning-disk confocal microscope (Dragonfly 200, Andor). The fluorescence intensity of C12-BODIPY inside *R. delemar* spores, which correlates with FFA accumulation, was quantified using IMARIS v.10.1 (Oxford Instruments Andor).

Assessment of C11-BODIPY uptake by *R. delemar* spores

C11-BODIPY (Invitrogen) was pre-oxidized by incubation in 20 mM H_2O_2/250 μM $CuSO_4$ in UV-grade ethanol at 37 °C under mild shaking for 48 h (ref. 82). As a negative control, an equal amount of C11-BODIPY (40 μM) was incubated in UV-grade ethanol under identical conditions. CFW-labelled *R. delemar* spores were incubated in RPMI/MOPS (pH 7) without phenol red, supplemented with either pre-oxidized C11-BODIPY or 2 μM control C11-BODIPY, at 37 °C in 18-well μ-Plates (Ibidi). After 4 h, spores were washed twice and imaged in PBS using a spinning-disk confocal microscope (Dragonfly 200, Andor). To validate probe oxidation, spores were first incubated with control C11-BODIPY for 4 h, washed with PBS to remove unbound dye and subsequently treated with increasing concentrations of H_2O_2 to induce lipid peroxidation. Oxidation was confirmed by a fluorescence shift from 590 nm (red) to 510 nm (green), proportional to the degree of lipid oxidation.

Uptake of oxidized OA by *R. delemar* spores

For the analysis of OA uptake by *R. delemar*, fungal spores were cultured in 5% ethanol/RPMI-MOPS supplemented with the indicated concentrations of OA (Sigma-Aldrich) or oxidized OA at 37 °C for 5 h. The spores were collected by scraping, collected in low-affinity 1.5 ml tubes, washed twice with PBS and fixed with methanol-free 4% formaldehyde at room temperature for 20 min. The spores were subsequently washed twice with PBS, stained with 0.5 μg ml^{-1} Nile red (Thermo Fisher Scientific) at room temperature for 20 min, washed again twice with PBS and stained with 200 μg ml^{-1} CFW at room temperature for 20 min. Flow cytometry data were acquired using the FACSCanto II system and analysed using FlowJo v.10.6 software (BD Biosciences). All images were acquired using a spinning disk confocal system (Dragonfly 200, Andor) equipped with a motorized inverted Nikon Eclipse Ti2-E microscope, an Andor Sona sCMOS 4.2B-6 camera and four laser lines (405 nm, 488 nm, 561 mm and 633 nm). All images were obtained through *z*-stacks, deconvolved with Fusion software v.2.3.0.44 (Andor, Oxford Instruments) and further processed in Imaris v.10.1 (Andor, Oxford Instruments) for contrast adjustment, area selection, colour combining and scale bar addition. Certain images were acquired with a Leica TCS SP8 confocal microscope with a ×63 lens and analysed with the use of Fiji/ImageJ. Low-fluorescence immersion oil (Nikon) was used, and imaging was performed at room temperature. Quantitative analysis of fluorescence in confocal microscopy images was performed with IMARIS v.10.1 (Oxford Instruments Andor).

Western blot analysis

The six elutions containing isolated HSA were subjected to western blot analysis for assessment of the isolation protocol. Immunoblotting was

performed according to the manufacturer's instructions using simultaneous antibodies against human transferrin and albumin at a 1:1,000 dilution, followed by incubation at 4 °C overnight. The appropriate secondary antibodies (HRP-conjugated anti-mouse IgG and anti-goat IgG) were used at a 1:5,000 dilution for 1 h at room temperature, and immunoblots were developed by chemiluminescence (ECL; Thermo Scientific). BlueStar Plus Prestained Protein Marker (NIPPON Genetics) was used for the evaluation of protein molecular mass and images were acquired using the ChemiDoc XRSImager (BioRad) system.

Antibodies

Anti-mucoricin and anti-CotH3 antibodies were generated as previously described[9]. Antibodies against human albumin (sc-365871) and transferrin (sc-365871) were purchased from Santa Cruz. An antibody against mouse active caspase-3 was purchased from Cell Signaling (9661).

Statistical analysis

For univariate and multivariate analysis of the prognostic value of albumin in mucormycosis the primary outcome was all-cause mortality from the time of diagnosis of the infection in the two cohorts at the MDACC, USA and PGIMER, Chandigarh, India and from the time of inclusion to the end of participation of patients (S24 visit) in the Ambizygo study, France. Categorical variables were compared by χ^2 or Fisher's exact test, as appropriate. Continuous variables were compared using the Wilcoxon rank-sum test. Univariate time-dependent survival analysis was performed for the main variables of interest (for example, severe hyperglycaemia, persistent neutropenia, severe hypoalbuminaemia, status of underlying malignancy, steroid use) using Kaplan–Meier curves and the Cox model. The multivariate Cox model was used to identify independent prognostic factor of mortality. Therefore, variables with a $P < 0.20$ on univariate analysis were included in an initial multivariate model that was then reduced to the final model by backward elimination. Kaplan–Meier survival curves were generated and compared between patients with different albumin levels using the log-rank test. All tests were two-sided with a significance level of 0.05. Data analysis and visualization were performed using Microsoft Office Excel 365 (Microsoft), Prism v10 (GraphPad), SAS v.9.4 (SAS Institute), R (v.4.3.1, R Core Team) and SPSS (IBM, SPSS Statistics for Windows, v.22.0).

For serum lipidomics analysis in $Alb^{-/-}$ and $Alb^{+/+}$ mice, significant differences between groups were assessed using the Wilcoxon rank-sum test. Data were row-centred and scaled, and visualized as heat maps using the pheatmap R package[75]. All other statistical analyses were performed using Prism v.10 (GraphPad) unless otherwise stated. $P < 0.05$ was considered statistically significant for all of the variables tested. A nonlinear regression three-parameter model—log(inhibitor) versus response (three parameters) was used to calculate IC_{50} values, according to the equation: $Y = \text{bottom} + (\text{top} - \text{bottom})/(1 + 10^{(X - \log[IC_{50}])})$. The FFA concentrations applied to generate the dose–response curves were based on physiological serum concentrations of each FFA in humans[24]. The statistical methods used to determine significance and the P values of each graph are provided in the figure legends.

Illustrations in Figs. 1f, 2a, 4a,f and 5d, and Extended Data Figs. 1b and 3a were created using BioRender.

Reporting summary

Further information on research design is available in the Nature Portfolio Reporting Summary linked to this article.

Data availability

All of the raw sequencing reads from this study are available at the NCBI Sequence Read Archive (SRA) under BioProject accession number PRJNA1141971. All data supporting the findings of this study are provided in the Article and its Supplementary Information. Source data are provided with this paper.

Code availability

No new code was generated for this study.

48. Chamilos, G. et al. *Drosophila melanogaster* as a model host to dissect the immunopathogenesis of zygomycosis. *Proc. Natl Acad. Sci. USA* **105**, 9367–9372 (2008).
49. Mertens, J. A., Skory, C. D. & Ibrahim, A. S. Plasmids for expression of heterologous proteins in *Rhizopus oryzae*. *Arch. Microbiol.* **186**, 41–50 (2006).
50. Kawakami, A. et al. Identification and characterization of oxidized human serum albumin: a slight structural change impairs its ligand-binding and antioxidant functions. *FEBS J.* **273**, 3346–3357 (2006).
51. Day, J. F., Thorpe, S. R. & Baynes, J. W. Nonenzymatically glucosylated albumin. In vitro preparation and isolation from normal human serum. *J. Biol. Chem.* **254**, 595–597 (1979).
52. Soliman, S. S. M. et al. Effective targeting of breast cancer cells (MCF7) via novel biogenic synthesis of gold nanoparticles using cancer-derived metabolites. *PLoS ONE* **15**, e0240156 (2020).
53. Semreen, M. H. et al. Metabolic profiling of candida auris, a newly-emerging multi-drug resistant *Candida* species, by GC-MS. *Molecules* **24**, 399 (2019).
54. Xia, J. & Wishart, D. S. Metabolomic data processing, analysis, and interpretation using MetaboAnalyst. *Curr. Protoc. Bioinformatics* https://doi.org/10.1002/0471250953.bi1410s34 (2011).
55. Alsabeeh, N., Chausse, B., Kakimoto, P. A., Kowaltowski, A. J. & Shirihai, O. Cell culture models of fatty acid overload: problems and solutions. *Biochim. Biophys. Acta* **1863**, 143–151 (2018).
56. Evans, M. et al. Conjugated linoleic acid suppresses triglyceride accumulation and induces apoptosis in 3T3-L1 preadipocytes. *Lipids* **35**, 899–910 (2000).
57. Ferraz, T., Fiuza, M., Dos Santos, M., De Carvalho, L. P. & Soares, N. M. Comparison of six methods for the extraction of lipids from serum in terms of effectiveness and protein preservation. *J. Biochem. Biophys. Methods* **58**, 187–193 (2004).
58. Yamazaki, E., Inagaki, M., Kurita, O. & Inoue, T. Kinetics of fatty acid binding ability of glycated human serum albumin. *J. Biosci.* **30**, 475–481 (2005).
59. Ekundayo, J. A. & Carlile, M. J. The germination of sporangiospores of *Rhizopus arrhizus*; spore swelling and germ-tube emergence. *J. Gen. Microbiol.* **35**, 261–269 (1964).
60. Schindelin, J. et al. Fiji: an open-source platform for biological-image analysis. *Nat. Methods* **9**, 676–682 (2012).
61. Ioannou, P. et al. Albumin enhances caspofungin activity against aspergillus species by facilitating drug delivery to germinating hyphae. *Antimicrob. Agents Chemother.* **60**, 1226–1233 (2015).
62. Davison, A. & Wajda, M. Analysis of lipids from fresh and preserved adult human brains. *Biochem. J.* **82**, 113 (1962).
63. Rose, H. G. & Oklander, M. Improved procedure for the extraction of lipids from human erythrocytes. *J. Lipid Res.* **6**, 428–431 (1965).
64. Srinivasan, A. et al. Microwave-enhanced advanced oxidation treatment of lipids and food wastes. *Water Air Soil Pollut.* **229**, 227 (2018).
65. Iuchi, K., Ema, M., Suzuki, M., Yokoyama, C. & Hisatomi, H. Oxidized unsaturated fatty acids induce apoptotic cell death in cultured cells. *Mol. Med. Rep.* **19**, 2767–2773 (2019).
66. Ghannoum, M. A., Filler, S. G., Ibrahim, A. S., Fu, Y. & Edwards, J. E. Jr. Modulation of interactions of *Candida albicans* and endothelial cells by fluconazole and amphotericin B. *Antimicrob. Agents Chemother.* **36**, 2239–2244 (1992).
67. Donnelly, J. P. et al. Revision and update of the consensus definitions of invasive fungal disease from the European Organization for Research and Treatment of Cancer and the Mycoses Study Group Education and Research Consortium. *Clin. Infect. Dis.* **71**, 1367–1376 (2020).
68. Dobin, A. et al. STAR: ultrafast universal RNA-seq aligner. *Bioinformatics* **29**, 15–21 (2013).
69. Liao, Y., Smyth, G. K. & Shi, W. featureCounts: an efficient general purpose program for assigning sequence reads to genomic features. *Bioinformatics* **30**, 923–930 (2014).
70. Love, M. I., Huber, W. & Anders, S. Moderated estimation of fold change and dispersion for RNA-seq data with DESeq2. *Genome Biol.* **15**, 550 (2014).
71. Subramanian, A. et al. Gene set enrichment analysis: a knowledge-based approach for interpreting genome-wide expression profiles. *Proc. Natl Acad. Sci. USA* **102**, 15545–15550 (2005).
72. Garcia Lopez, A., Albrecht-Eckardt, D., Panagiotou, G. & Schäuble, S. FungiFun3: systemic gene set enrichment analysis for fungal species. *Bioinformatics* **40**, btae620 (2024).
73. Kanehisa, M., Sato, Y. & Morishima, K. BlastKOALA and GhostKOALA: KEGG tools for functional characterization of genome and metagenome sequences. *J. Mol. Biol.* **428**, 726–731 (2016).
74. Luo, W., Friedman, M. S., Shedden, K., Hankenson, K. D. & Woolf, P. J. GAGE: generally applicable gene set enrichment for pathway analysis. *BMC Bioinformatics* **10**, 161 (2009).
75. Kolde, R. & Kolde, M. R. pheatmap. R package version 1.0.12 (CRAN, 2015).
76. Luo, G. et al. Efficacy of liposomal amphotericin B and posaconazole in intratracheal models of murine mucormycosis. *Antimicrob. Agents Chemother.* **57**, 3340–3347 (2013).
77. Wurster, S. et al. Blockade of the PD-1/PD-L1 immune checkpoint pathway improves infection outcomes and enhances fungicidal host defense in a murine model of invasive pulmonary mucormycosis. *Front. Immunol.* **13**, 838344 (2022).
78. Chamilos, G. et al. *Candida albicans* Cas5, a regulator of cell wall integrity, is required for virulence in murine and toll mutant fly models. *J. Infect. Dis.* **200**, 152–157 (2009).
79. Stolz, D. J., Sands, E. M., Amarsaikhan, N., Tsoggerel, A. & Templeton, S. P. Histological quantification to determine lung fungal burden in experimental aspergillosis. *J. Vis. Exp.* **9**, 57155 (2018).
80. Varma, S. G., Mitra, A. & Sarkar, S. Self-diffusion is temperature independent on active membranes. *Phys. Chem. Chem. Phys.* **26**, 23348–23362 (2024).

81. Tomoda, H., Kishimoto, Y. & Lee, Y. C. Temperature effect on endocytosis and exocytosis by rabbit alveolar macrophages. *J. Biol. Chem.* **264**, 15445–15450 (1989).
82. Drummen, G. P., Gadella, B. M., Post, J. A. & Brouwers, J. F. Mass spectrometric characterization of the oxidation of the fluorescent lipid peroxidation reporter molecule C11-BODIPY(581/591). *Free Radic. Biol. Med.* **36**, 1635–1644 (2004).

Acknowledgements We thank E. Deligianni for assistance with time-lapse microscopy; K. Stylianou, C. Tsatsanis and M. Katrinaki for providing reagents and human samples, and performing measurements of albumin levels in human and mouse serum samples; A. Vatikioti for assistance with mouse sera collection; and I. Lagkouvardos for discussions and input on RNA-seq data analysis. A.P. was supported by the General Secretariat for Research and Technology (GSRT) and the Hellenic Foundation for Research and Innovation (H.F.R.I.) under the "1st call of H.F.R.I. for PhD Candidates" (project number: 1119); I.M. by the Hellenic Foundation for Research and Innovation (H.F.R.I.) under the "3rd Call for H.F.R.I. Research Projects to support Post-Doctoral Researchers" (project number: 7054); G.C. by an ERC Consolidator Grant (iMAC-FUN, 864957), an Horizon 2020–Research and Innovation Framework Programme from Europe, H2020-SC1-BHC-2018-2020 (HDM-FUN, 84750) and a 'la Caixa' Foundation Health Research Grant (TRANS-CPA, LCF/PR/HR17/52190003); G.C., E.K., A.E. and K.G. by the General Secretariat for Research and Innovation of Greece Grant PRO-sCAP (project code TAEDR-0541976) carried out within the framework of the National Recovery and Resilience Plan Greece 2.0 and funded by the European Union-Next Generation EU; A.C. by the Fundação para a Ciência e a Tecnologia (FCT) (UID/06304/2023, LA/P/0050/2020 and 2022.06674.PTDC) and by the 'la Caixa' Foundation under the agreement LCF/PR/HR22/52420003; V.G. and C.L. by the grant PID2024-160088NB-I00 funded by MICIU/AEI/10.13039/501100011033 and by ERDF/EU; A.S.I by the Public Health Service grant no. R01 AI063503; and V.M.B. by NIH grants U19 AI110820 and R01AI141360. D.P.K. acknowledges the Robert C. Hickey endowment.

Author contributions A.P., I.M. and V.N. performed and analysed most of the experiments in human samples and mice and participated in writing the manuscript. I.M. established protocols on the in vivo model of invasive fungal infections in albumin-KO mice, and in vitro assays on the assessment of antimicrobial activity of serum and BAL lipids and fungal protein synthesis. R.H. and S.S.M.S. analysed vitamins, trace elements and amino acids in culture medium, performed chemical modifications of albumin and serum lipids, and validated the efficiency of oxidation of FFAs. A.L.-L., M.M.-G. and S.M.C.-A. performed lipidomics analyses. V.M., R.A., S.M.R., F.L. and A.C. collected and analysed clinical data. M.H. and V.P. performed fractionation and identification of FFAs in albumin samples. M.P. and K.P. established the assays for human albumin depletion and purification from serum. I.K. performed in vivo studies and analysed data. Y.G. performed experiments on mucoricin expression and provided reagents. R.A., T.M., Y.V. and J.M. provided human samples and analysed data. S.-Y.C. and A.S. analysed clinical data. D.S. and E.K. collected human serum samples and analysed data. A.E. and K.G. analysed data. A.C. analysed data. O.K. provided clinical isolates and analysed data. E.D. and M.T. performed histopathological studies. V.M.B. performed RNA-seq analyses. E.I. performed gene enrichment analysis of RNA-seq data and analysed lipidomics data. V.G. and C.L. supervised the analysis on fungal transcriptomics. Y.J. and C.E. performed logistic regression analysis of clinical cohorts. C.B. supervised all of the lipidomics studies. D.P.K. provided clinical data and suggestions throughout the study. A.S.I. provided reagents, designed and supervised experiments, analysed data and participated in discussions and suggestions throughout the study. G.C. conceived and supervised the study, was involved in the design and evaluation of all of the experiments, and wrote the manuscript along with comments from all of the other authors.

Competing interests A.S.I. owns shares in Vitalex Biosciences, a start-up company that is developing immunotherapies and diagnostics for mucormycosis. The other authors declare no competing interests.

Additional information
Supplementary information The online version contains supplementary material available at https://doi.org/10.1038/s41586-025-09882-3.
Correspondence and requests for materials should be addressed to Georgios Chamilos.
Peer review information *Nature* thanks Andrew Hall, Tobias Hohl and the other, anonymous, reviewer(s) for their contribution to the peer review of this work. Peer reviewer reports are available.

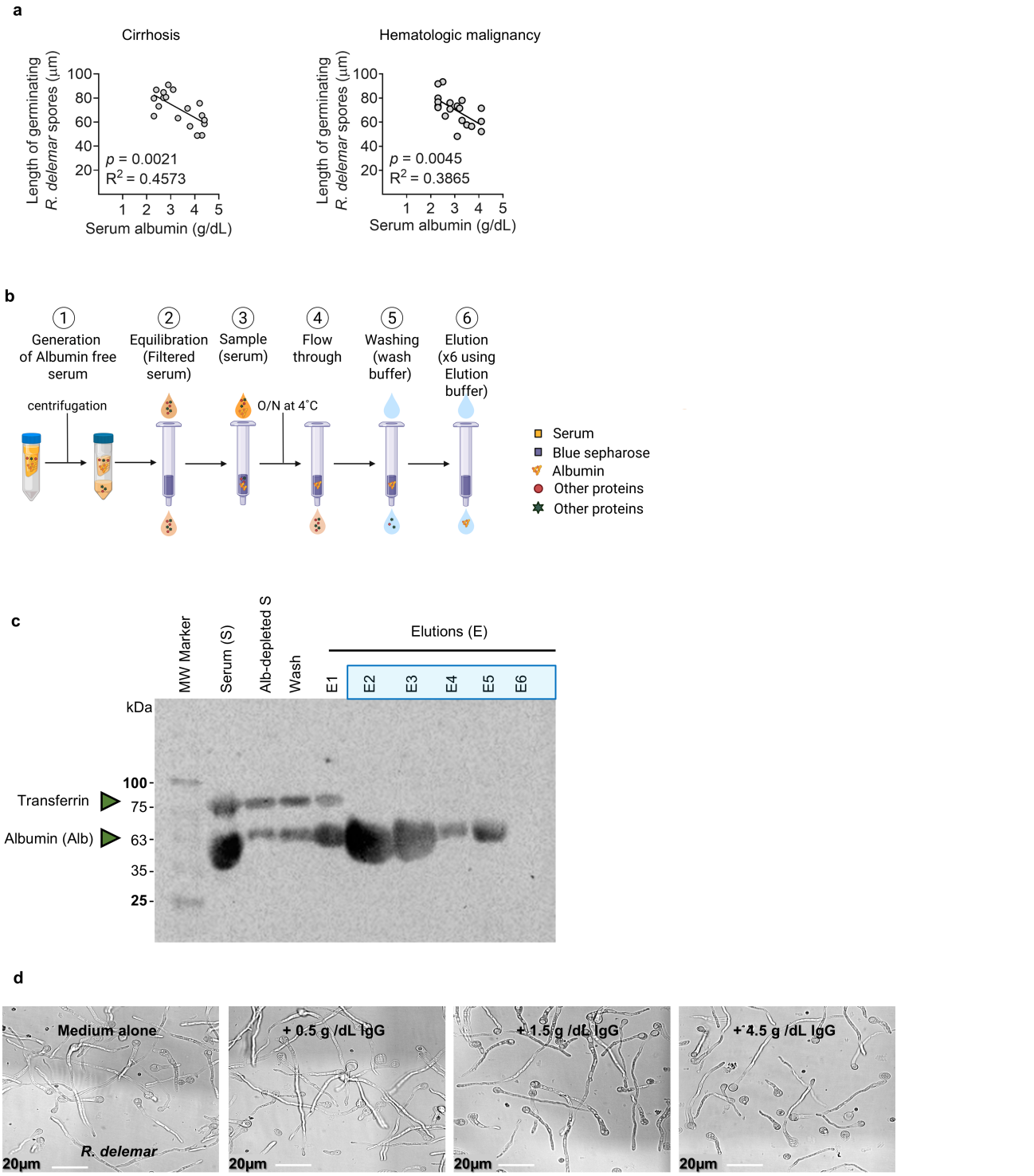

Extended Data Fig. 1 | Correlation of serum albumin level with antifungal activity, albumin purification, and evaluation of other serum proteins. **a**, Correlation between serum albumin levels and *R. delemar* growth in human sera obtained from patients with cirrhotic disease (n = 18, left) or haematologic malignancies (n = 20, right). Simple linear regression test was used to determine deviation from zero. **b**, Outline of human serum isolation using blue Sepharose columns. **c**, Immunoblot analysis of albumin and transferrin in human serum and eluted fragments following isolation. Representative image from 3 independent experiments. **d**, Representative images of *R. delemar* spores cultured for 8 h in medium alone or medium supplemented with increasing concentrations of human IgG. Representative images from 3 independent experiments performed in triplicate. Scale bar, 20 µm.

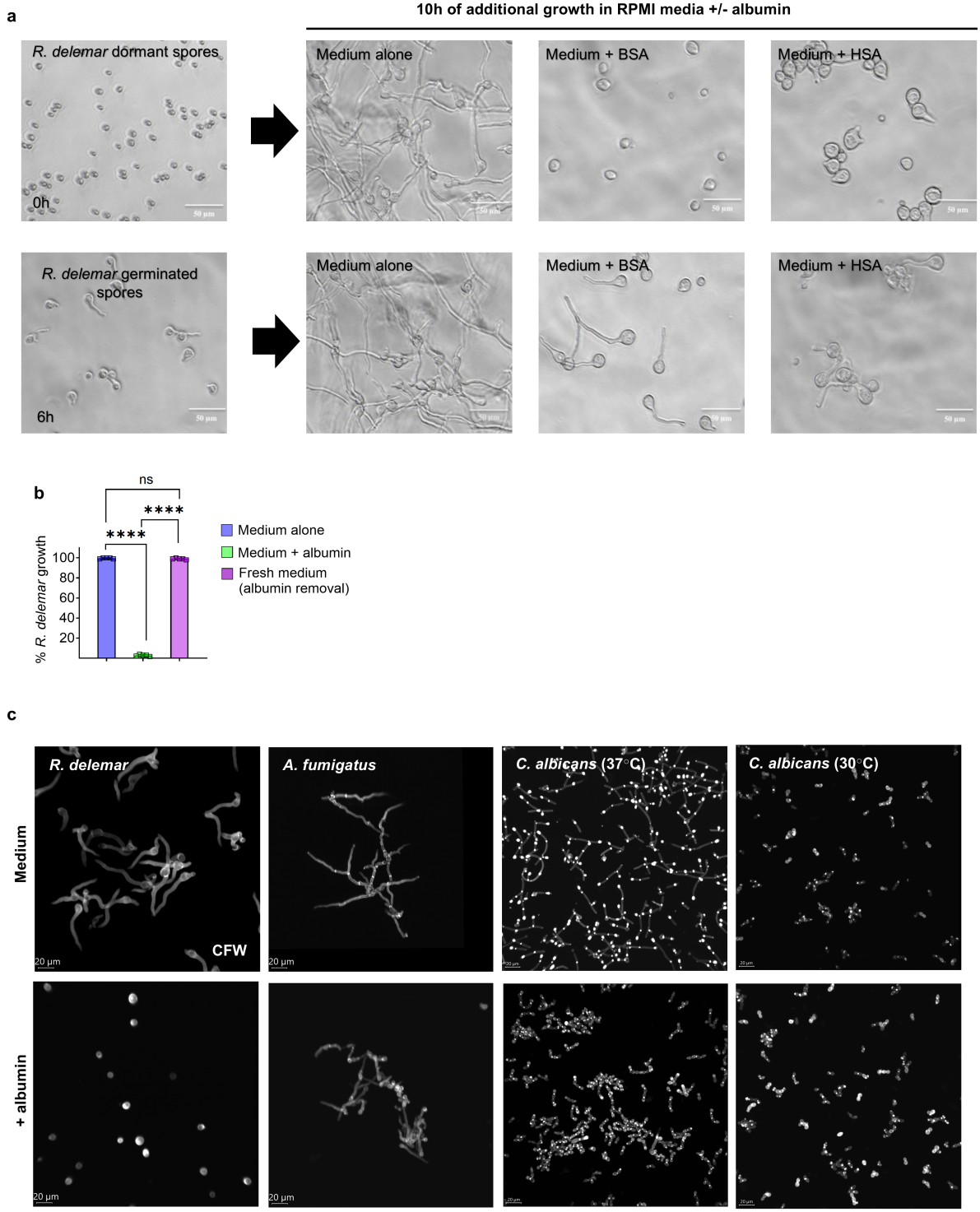

Extended Data Fig. 2 | Selective fungistatic activity of albumin against Mucorales. a, Representative images of *R. delemar* dormant spores (upper panel) or germinating spores (lower panel) cultured for 10 h in medium alone, medium + BSA, or medium + HSA. Scale bar, 50 µm. **b**, Assessment of *R. delemar* germination in medium alone, medium supplemented with human serum albumin (medium + albumin), or medium alone following initial incubation in albumin-containing medium (fresh medium) (n = 5 independent experiments). Data are mean ± s.d. ns = 0.437; ****$p < 0.0001$, one-way ANOVA with Tukey's multiple comparisons post hoc test. **c**, Representative fluorescence images of different human fungal pathogens labelled with CFW-and cultured for 6 h in medium ± 4.5 g dl^{-1} albumin. Scale bar, 20 µm.

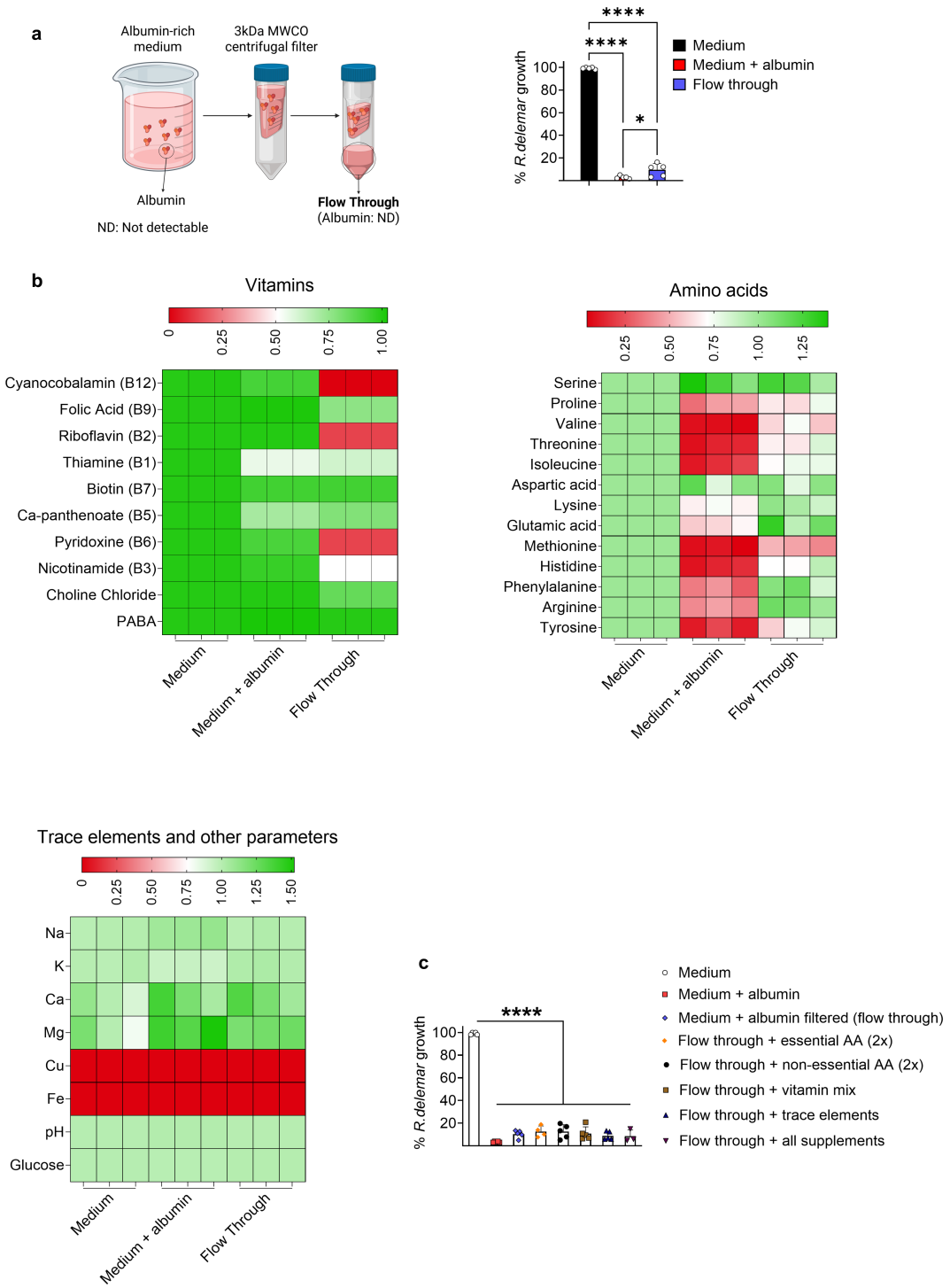

Extended Data Fig. 3 | Analysis of antifungal activity and composition of albumin-rich medium following filtration. a, Outline of albumin-rich medium filtration and generation of albumin-depleted flow through (left panel; created with BioRender.com). Assessment of *R. delemar* growth in medium, medium + albumin, or medium + albumin-depleted flow through (right panel) (n = 5 independent experiments). Data are mean ± s.d. *p = 0.022; ****p < 0.0001, one-way ANOVA with Tukey's test. **b**, Heatmap of vitamins, amino acids (LC-MS), and trace elements (ICP-MS). Standard RPMI set to 1; red = low, green = high. **c**, Assessment of *R. delemar* growth in medium ± albumin (n = 3) and medium + flow through ± essential/non-essential amino acids (n = 3), vitamins, trace elements (n = 3), or all combined (n = 3), from independent experiments performed in triplicate. Data are mean ± s.d. ****p < 0.0001, one-way ANOVA with Tukey's test. Data are included in Source Data file.

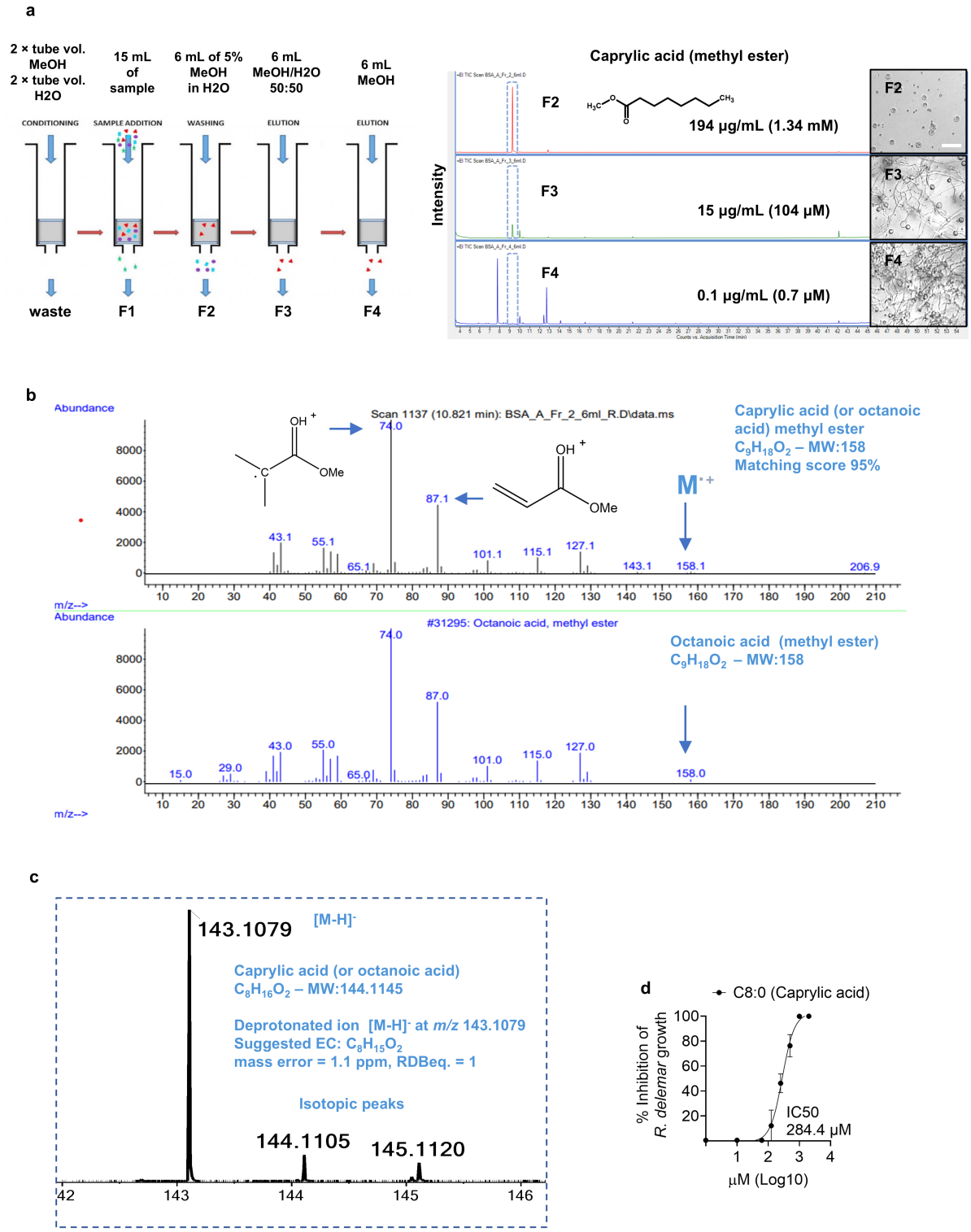

Extended Data Fig. 4 | Analysis of activity and FFA composition in albumin filtrate. a, Outline of solid-phase extraction (SPE) procedure. GC-MS TIC chromatographs of derivatized fractions (F2–F4) and assessment of *R. delemar* growth (16 h). Scale bar, 50 µm. Caprylic acid concentrations: F2 = 194 µg/mL (1.34 mM), F3 = 15 µg/mL (104 µM), F4 = 0.1 µg/mL (0.7 µM). **b**, EI-MS spectrum of F2 (caprylic acid methyl ester) compared to NIST14.0 reference. Molecular ion ($M^{+\cdot}$, m/z 158) and characteristic fragments annotated. **c**, ESI(-)-TOF-MS of underivatized F2: $[M-H]^-$ at m/z 143.1079 with isotopic distribution; EC and RDB eq. provided. Data are a representative example of n = 2 independent experiments. **d**, Inhibition of *R. delemar* by increasing purified caprylic acid in 5% EtOH (n = 6 independent experiments). Data are mean ± s.d.

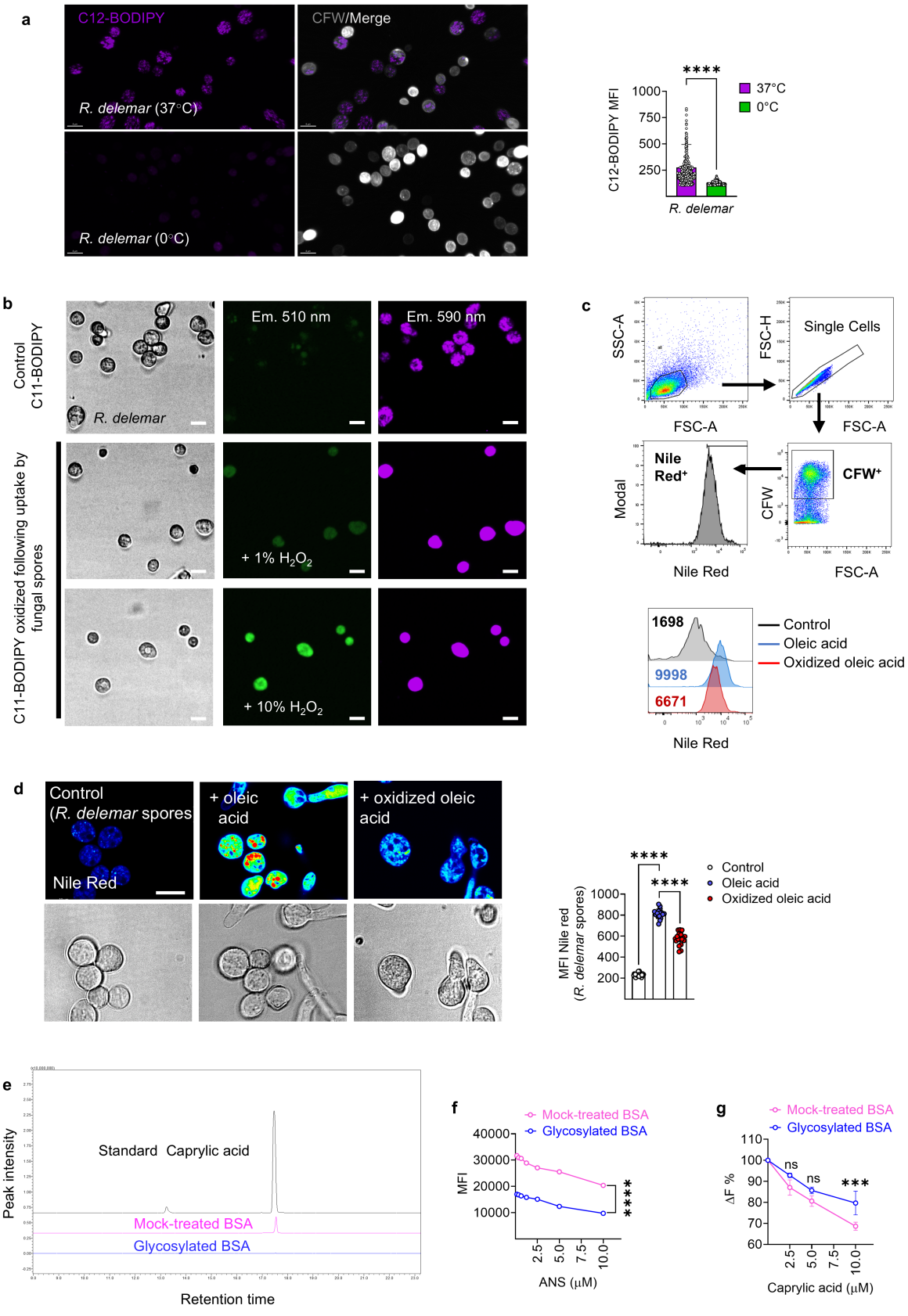

Extended Data Fig. 5 | Active uptake of non-oxidized FFAs by Mucorales. **a**, Representative fluorescence images and cumulative C12-BODIPY MFI of CFW-labelled *R. delemar* spores at 37 °C or 0 °C (n = 316–334 spores, 3 independent experiments). Data are mean ± s.d. ****p < 0.0001, Mann–Whitney test. **b**, Fluorescence of *R. delemar* spores cultured with C11-BODIPY ± 0%, 1%, or 10% H_2O_2 (3 independent experiments). Scale bar, 10 μm. **c**–**d**, Nile Red staining of spores in medium ± oleic acid or oxidized OA. Representative images and cumulative MFI (n = 25–20 optical fields, 3 experiments). Data are mean ± s.d. ****p < 0.0001, one-way ANOVA with Tukey's test. **e**–**g**, GC-MS, ANS binding, and fluorescence quenching of caprylic acid on glycosylated/non-glycosylated BSA (n = 3 independent experiments). Data are mean ± s.d. **p-values as indicated.

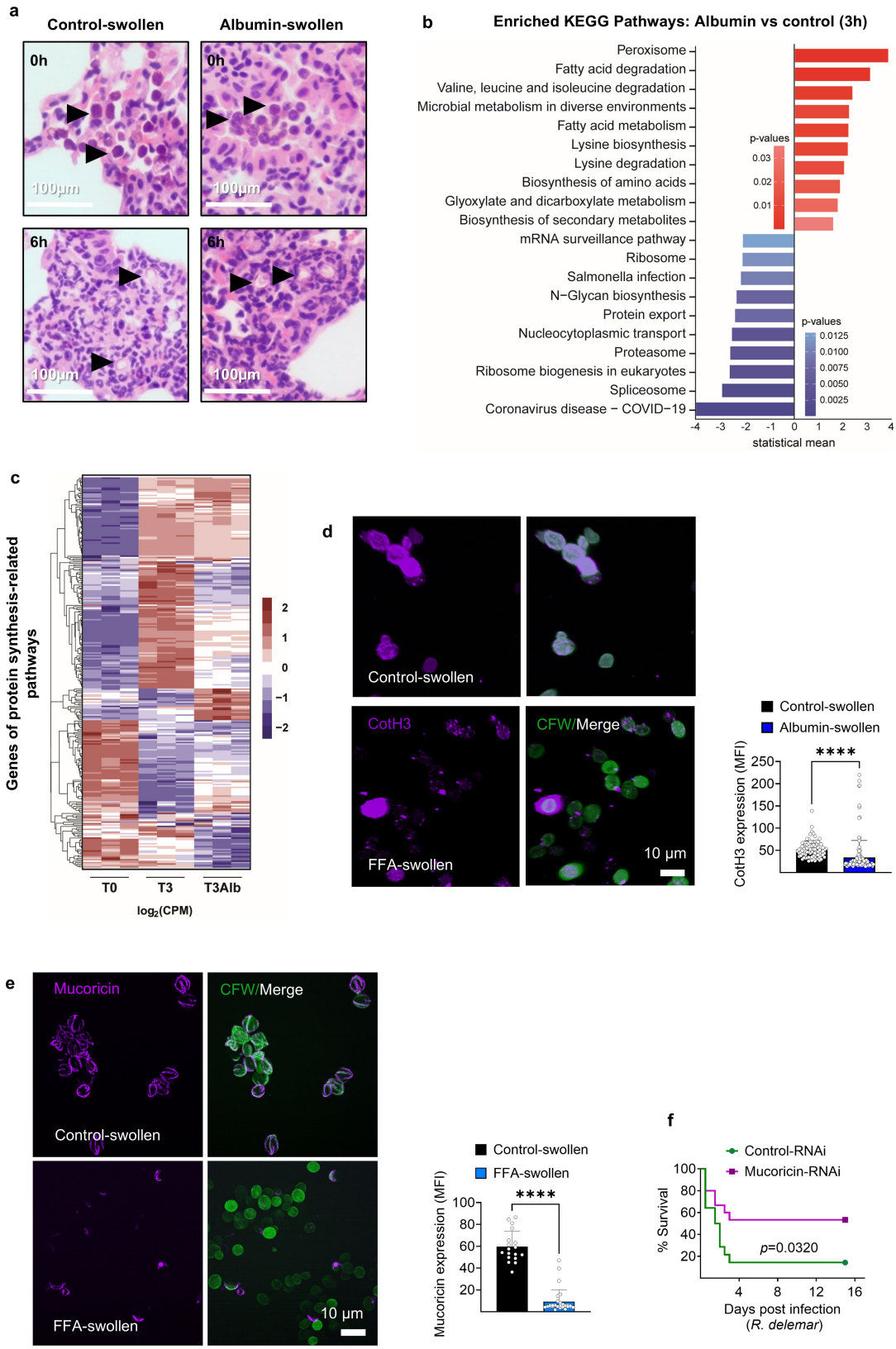

Extended Data Fig. 6 | Albumin-bound FFAs suppress Mucorales virulence via protein synthesis arrest. a, H&E histopathology of lungs at 0 h and 6 h post-infection with control (n = 8)- or albumin-swollen (n = 7) *R. delemar*. Scale bar, 100 µm. **b**, Enriched KEGG pathways for DEGs (GSEA). **c**, Differential expression of protein synthesis-related genes in dormant spores (T0) or after 3 h in medium ± albumin (T3/T3Alb) (n = 3 biologically independent samples). **d**–**e**, Representative confocal images and cumulative data for CotH3 and mucoricin expression (n = 85–128 spores or 18–29 optical fields, 3 independent experiments). Data are mean ± s.d. ****$p < 0.0001$, Mann–Whitney test. **f**, Survival of C57BL/6 mice infected i.t. with 2.5×10^6 swollen control-RNAi (n = 14) or mucoricin-RNAi (n = 15) spores. Log-rank (Mantel–Cox) test.

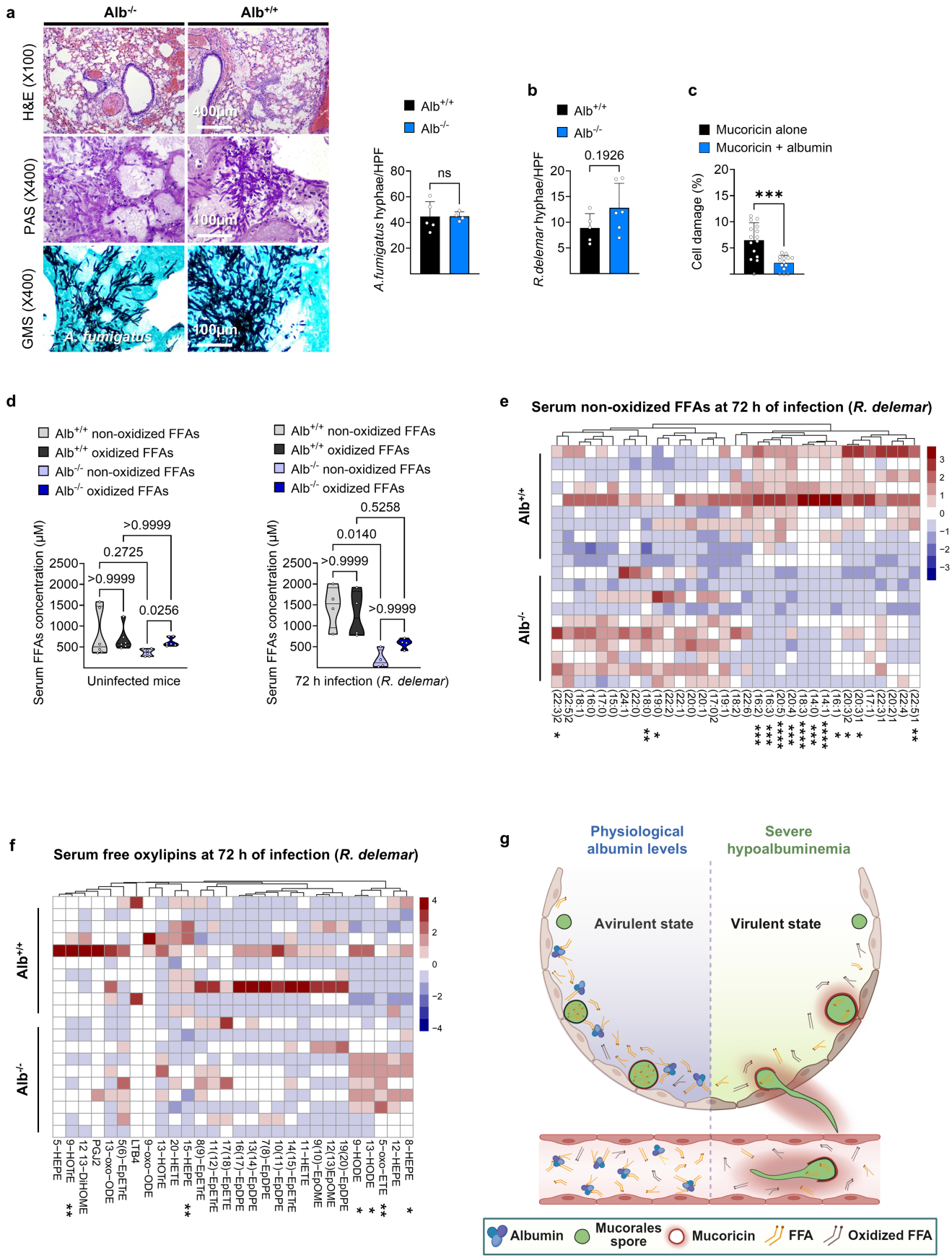

Extended Data Fig. 7 | See next page for caption.

Extended Data Fig. 7 | Albumin deficiency compromises serum FFA composition and increases susceptibility to mucormycosis. **a**–**b**, Histopathology and cumulative hyphal counts of lungs from neutropenic $Alb^{+/+}$ and $Alb^{-/-}$ mice infected with *A. fumigatus* or *R. delemar* (n = 4–6 mice). Data are mean ± s.d., two-sided Mann–Whitney test. Scale bar, 100 µm. **c**, Cell damage of A549 cells treated with mucoricin ± 4.5 g dl^{-1} FFA-free BSA (n = 14 mucoricin plus BSA, n = 15 mucoricin alone). Data are mean ± s.d. ***p = 0.0004, Mann–Whitney test. **d**, Serum non-oxidized/oxidized FFA concentrations in uninfected and infected $Alb^{+/+}$ vs $Alb^{-/-}$ mice (n = 6). One-way ANOVA with Dunn's test. **e**–**f**, Heatmaps of serum FFAs and free oxylipins (n = 10 mice, Wilcoxon rank sum test). **g**, Proposed model of albumin in host defence during Mucorales infection. Created with BioRender.com.

Extended Data Table 1 | Cox regression analysis of mortality in patients with pulmonary mucormycosis from the MDACC, USA cohort (n=81)

	Cox regression analysis on 42-day mortality				Cox regression analysis on 84-day mortality			
	UV analysis		MV analysis		UV analysis		MV analysis	
Variables	**cHR (95% CI)**	***p*-value**	**aHR (95% CI)**	***p*-value**	**cHR (95% CI)**	***p*-value**	**aHR (95% CI)**	***p*-value**
Persistent neutropenia*	3.85 (2.03 - 7.29)	< .0001	3.94 (2.08 - 7.49)	< .0001	4.16 (2.36 - 7.33)	< .0001	4.34 (2.45 - 7.70)	< .0001
Steroid use (prednisone ≥ 600 mg) in one month before diagnosis	1.14 (0.60 – 2.19)	0.686	- #		0.96 (0.54 - 1.70)	0.876	- #	
Status of hematological malignancy		0.213	- #			0.046	- #	
Active	1.81 (0.71 - 4.63)				2.38 (1.01 - 5.56)			
In remission	Reference				Reference			
Severe hyperglycemia	1.09 (0.54 - 2.24)	0.806	- #		1.11 (0.59 - 2.07)	0.745	- #	
Albumin at diagnosis		0.015		0.012		0.034		0.019
≤ 2.5	2.19 (1.17 - 4.11)		2.26 (1.20 - 4.25)		1.82 (1.05 - 3.18)		1.95 (1.12 - 3.41)	
> 2.5	Reference				Reference			

Abbreviations: cHR= Crude Hazard ratio; aHR= Adjusted Hazard ratio; 95% CI= 95% Confidence interval; UV analysis= Univariable analysis; MV analysis= Multivariable analysis.

Notes: * Persistent neutropenia indicates neutropenia at infection diagnosis without recovery during follow-up. # Variable was removed from the final multivariable model due to lack of statistical significance (p >0.05).

Persistent neutropenia and severe hypoalbuminemia (serum albumin ≤ 2.5 g dl^{-1}) were identified as independent predictors of 42-day and 84-day mortality in multivariable analysis.

Extended Data Table 2 | Cox regression analysis of 90-day mortality in patients with pulmonary mucormycosis from the PGIMER, Chandigarh, India cohort (n=100), including a subgroup analysis of 83 patients with diabetes mellitus

	Cox regression analysis on 90-day mortality *(entire cohort)				Cox regression analysis on 90-day mortality †(diabetes mellitus cohort)			
	UV analysis		MV analysis		UV analysis		MV analysis	
Variables	**cHR (95% CI)**	***p*-value**	**aHR (95% CI)**	***p*-value**	**cHR (95% CI)**	***p*-value**	**aHR (95% CI)**	***p*-value**
Age, years	0.99 (0.96-1.01)	0.27			0.99 (0.96-1.03)	0.71		
Sex	0.92 (0.46-1.84)	0.81			0.71 (0.31-1.66)	0.44		
COVID-19	0.90 (0.38-2.13)	0.80			1.04 (0.43-2.56)	0.93		
Risk factor					-			
Diabetes	Reference				-			
Transplantation	1.63 (0.72-3.71)	0.25			-			
Others	2.68 (0.94-7.62)	0.06			-			
Albumin at diagnosis		**0.0001**		**0.001**		**0.0001**		**0.0001**
> 2.5	Reference				Reference			
≤ 2.5	3.17 (1.70 – 5.91)		3.06 (1.61 – 5.82)		3.76 (1.79-7.93)		4.14 (1.94 – 8.83)	
Surgery for PM	0.21 (0.07-0.68)	**0.009**	0.21 (0.07-0.71)	**0.011**	0.32 (0.10-1.05)	0.06	0.30 (0.09-1.01)	0.05

The 90-d mortality data was available for 100 participants *(complete cohort) and †83 participants in the diabetes mellitus only cohort
Abbreviations: aHR= Adjusted Hazard ratio; 95% CI= 95% Confidence interval. cHR= Crude Hazard ratio; PM: pulmonary mucormycosis

Severe hypoalbuminemia (serum albumin ≤ 2.5 g dl^{-1}; p=0.001; aHR = 3.06, 95% CI=1.61–5.82) and surgery for pulmonary mucormycosis (p=0.01; aHR = 0.21, 95% CI=0.07–0.71) were independent predictors of 90-day mortality. Severe hypoalbuminemia remained independently associated with mortality among patients with diabetes mellitus (p=0.0001; aHR = 4.14, 95% CI=1.94–8.83).

Extended Data Table 3 | Cox regression analysis of mortality in patients with pulmonary mucormycosis from the AmbiZygo, France cohort (n=26)

	Cox regression analysis			
		UV analysis	MV analysis	
Variables	**cHR (95% CI)**	***p*-value**	**aHR (95% CI)**	***p*-value**
Age (continuous)	1.01 (0.98-1.04)	0.55		
Age ≤50	1.43 (0.48-4.23)	0.52		
Age >50	Reference			
Sex				
Female	0.68 (0.21-2.16)	0.51		
Male	Reference			
Curative surgery before treatment	0.96 (0.34-2.74)	0.94		
Diabetes	0.85 (0.27-2.72)	0.78		
BMI ≥ 25	1.16 (0.32-4.21)	0.83		
Underlying condition				
Other	Reference			
H.M. or other Ca[1*]	5.30 (1.45-19.36)	0.012	3.70 (0.98, 14.04)	0.054
Albumin				
Albumin > 2.5[2†]	0.57 (0.06-0.58)	0.004	0.27 (0.09-0.85)	0.025
Albumin ≤ 2.5	Reference			

*Hematologic malignancy or other malignancy; †Serum albumin level on diagnosis measured in g/dL, Underlying condition: Other included diabetes mellitus, trauma, diabetic ketoacidosis, solid organ transplant, or no underlying condition; BMI = body mass index
Abbreviations: aHR = Adjusted Hazard ratio; 95% CI = 95% Confidence interval. cHR = Crude Hazard ratio; H.M. = hematological malignancy, Ca = cancer

Serum albumin > 2.5 g dl^{-1} at diagnosis was identified as the only independent predictor of 24-week mortality in multivariable analysis (p=0.025; aHR = 0.27, 95% CI=0.09–0.80).

nature portfolio

Corresponding author(s): Georgios Chamilos

Last updated by author(s): Nov 6, 2025

Reporting Summary

Nature Portfolio wishes to improve the reproducibility of the work that we publish. This form provides structure for consistency and transparency in reporting. For further information on Nature Portfolio policies, see our Editorial Policies and the Editorial Policy Checklist.

Statistics

For all statistical analyses, confirm that the following items are present in the figure legend, table legend, main text, or Methods section.

n/a	Confirmed
☐	☒ The exact sample size (*n*) for each experimental group/condition, given as a discrete number and unit of measurement
☐	☒ A statement on whether measurements were taken from distinct samples or whether the same sample was measured repeatedly
☐	☒ The statistical test(s) used AND whether they are one- or two-sided *Only common tests should be described solely by name; describe more complex techniques in the Methods section.*
☒	☐ A description of all covariates tested
☐	☒ A description of any assumptions or corrections, such as tests of normality and adjustment for multiple comparisons
☐	☒ A full description of the statistical parameters including central tendency (e.g. means) or other basic estimates (e.g. regression coefficient) AND variation (e.g. standard deviation) or associated estimates of uncertainty (e.g. confidence intervals)
☐	☒ For null hypothesis testing, the test statistic (e.g. *F*, *t*, *r*) with confidence intervals, effect sizes, degrees of freedom and *P* value noted *Give P values as exact values whenever suitable.*
☒	☐ For Bayesian analysis, information on the choice of priors and Markov chain Monte Carlo settings
☒	☐ For hierarchical and complex designs, identification of the appropriate level for tests and full reporting of outcomes
☒	☐ Estimates of effect sizes (e.g. Cohen's *d*, Pearson's *r*), indicating how they were calculated

Our web collection on statistics for biologists contains articles on many of the points above.

Software and code

Policy information about availability of computer code

Data collection

All Images were acquired using a spinning disk confocal system (Dragonfly 200, Andor) equipped with motorized inverted Nikon Eclipse Ti2-E microscope, the Andor Sona sCMOS 4.2B-6 camera, and four laser lines (405nm, 488nm, 561nmm and 633nm). All images were obtained using z-stacks, then deconvolved with the Fusion software version 2.3.0.44 (Andor, Oxford Instruments). Certain images were acquired with a Leica TCS SP8 confocal microscope. Western blots were images were acquired using ChemiDoc XRSImager (Biorad). Acquisition of flow cytometry data was performed using a FACSCanto II system (BD Biosciences).
The quantification of amino acids was conducted via a standard mix calibration curve, via the UPLC-MS/MS system controlled by Lynx software (Version 4.1, SCN 882).

Data analysis

All images were acquired with the Fusion software version 2.3.0.44 (Andor, Oxford Instruments) and further processed in Imaris 10.1 (Andor – Oxford Instruments) for contrast adjustment, area selection, color combining and scale bar addition. Certain images were analyzed with the use of Fiji/Image J v1.54. Flow cytometry data were analyzed using FlowJo v10.6 Software (BD Sciences).
Metabolites obtained from chemically modified albumin were imported into MetaboAnalyst (v.5.0, https://www.metaboanalyst.ca/home.xhtml). Data analysis of amino acids in culture media was performed via the TargetLynx™ program. The raw data of FFAs collected by LC–MS were reprocessed with MassHunter Profinder software version B.10.02. RNA sequencing reads were aligned to the reference genome (R. delemar 99-880) using STAR aligner version 2.7.10. The reads that mapped to genomic features were calculated using the featureCounts program version 2.0.3. Statistical analysis of differential gene expression was performed using the DEseq2 R-based package. The gene ontology (GO) enrichment analysis performed using the Gene Set Enrichment Analysis (GSEA) method as previously implemented by the web-based application FungiFun3 (https://fungifun3.hki-jena.de/). The BlastKOALA automatic annotation server was used for the functional annotation and the assignment of the KEGG Orthologies (KOs). The pathway enrichment analysis performed using the Generally Applicable Gene-set Enrichment (GAGE) method and functions of the gage R-based package. The genes of the selected KEGG pathways were identified using the KEGG PATHWAY database. R programing language (4.3.1) was used for the visualization of the results. The heatmaps were produced

using the pheatmap package. Data analysis and visualization were performed using Microsoft Office Excel 365 (Microsoft Corporation), Prism v10 (GraphPad Software), SAS version 9.4 (SAS Institute Inc.) and SPSS (IBM SPSS Statistics for windows, version 22.0. Armonk, NY: IBM Corp).

For manuscripts utilizing custom algorithms or software that are central to the research but not yet described in published literature, software must be made available to editors and reviewers. We strongly encourage code deposition in a community repository (e.g. GitHub). See the Nature Portfolio guidelines for submitting code & software for further information.

Data

Policy information about availability of data

All manuscripts must include a data availability statement. This statement should provide the following information, where applicable:

- Accession codes, unique identifiers, or web links for publicly available datasets
- A description of any restrictions on data availability
- For clinical datasets or third party data, please ensure that the statement adheres to our policy

All of the raw sequencing reads from this study are available at the NCBI Sequence Read Archive (SRA) under BioProject accession number PRJNA1141971. The data generated during this study are provided as Source data and Supplementary data.

Research involving human participants, their data, or biological material

Policy information about studies with human participants or human data. See also policy information about sex, gender (identity/presentation), and sexual orientation and race, ethnicity and racism.

Reporting on sex and gender	All biological attributes related to sex and gender for patients included across the eight clinical cohorts are presented in Supplementary Table 1. For the AmbiZygo cohort of mucormycosis patients, detailed characteristics—including sex and gender—are reported in the original publication: Lanternier F, et al; French Mycosis Study Group. Prospective pilot study of high-dose (10 mg/kg/day) liposomal amphotericin B (L-AMB) for the initial treatment of mucormycosis. J Antimicrob Chemother. 2015 Nov;70(11):3116–23. doi:10.1093/jac/dkv236. Epub 2015 Aug 27. PMID: 26316385.
Reporting on race, ethnicity, or other socially relevant groupings	None of these characteristics were included in the data collected from the study.
Population characteristics	Detailed information on patient demographics, clinical characteristics, and albumin levels is provided in Supplementary Table 1. The relevant clinical information for patients in the AmbiZygo cohort of mucormycosis patients is available in the original publication (Lanternier, F. et al. Prospective pilot study of high-dose (10 mg/kg/day) liposomal amphotericin B (L-AMB) for the initial treatment of mucormycosis. J Antimicrob Chemother 70, 3116–3123 (2015). https://doi.org/10.1093/jac/dkv236).NCT00467883
Recruitment	The medical records of contemporaneous patients who had been admitted at the Leukemia Department of the MD Anderson Cancer Center were retrospectively reviewed. Standardized EORTC/MSG criteria were applied for diagnosis of pulmonary mucormycosis and pulmonary aspergillosis (Donnelly, J. P. et al. Revision and Update of the Consensus Definitions of Invasive Fungal Disease From the European Organization for Research and Treatment of Cancer and the Mycoses Study Group Education and Research Consortium. Clin Infect Dis 71, 1367–1376 (2020). https://doi.org/10.1093/cid/ciz1008). Clinical information of matched control patients for the underlying disease who developed bacterial (Legionella) pneumonia were also reviewed. Albumin levels were retrieved from the medical records of all the patients on the day of hospital admission. Information on demographics, underlying disease and risk factors for mucormycosis was collected. The study was approved by the IRB (IRB Protocol: PA14-0802) of the MDACC. The medical records of consecutive patients admitted to the Department of Pulmonary Medicine, Department of Medical Microbiology, Institute of Medical Education and Research (PGIMER), Sector-12, Chandigarh, 160012, India over the past 8 years (2016–2023) with a diagnosis of pulmonary mucormycosis were retrospectively evaluated. The study was approved by the Institutional Ethics Committee (IEC; Intramural; INT) of the PGIMER;(IEC/INT approval no: 2023/Study-1564) and registered with the Biological Research Regulatory Approval Portal (BIORRAP; registration no. POS36452025). All procedures were conducted in accordance with institutional and national guidelines. Serum samples were prospectively collected from healthy individuals, cirrhotic patients, and patients with hematological malignancies at the University Hospital of Heraklion, Crete, and the Therapeutics Clinic of the General Hospital of Athens “Alexandra”. Demographics, clinical characteristics and serum albumin level, total free fatty acid (FFA) and oxidized FFA levels were measured in the sera of healthy individuals and patients. Approval for the collection of clinical information and blood samples from all individuals mentioned above was obtained from the Ethics Committee of the University of Heraklion, Crete, Greece (5159/2014, 10925/201 and 13-04-22/7970) and Therapeutics Clinic (122/18-2-2021). All patients were fully informed and provided written informed consent in accordance with the Declaration of Helsinki. For lipidomic and functional studies, serum samples from patients with mucormycosis, or invasive pulmonary aspergillosis and matched control patients were obtained from hematological malignancy patients admitted to the University Hospitals of Leuven, Belgium (IRB# S61797). All study participants were recruited through institutional internal channels. Although there may be a bias toward individuals of White ethnicity (Greek, Belgian), this is considered unlikely to impact the study outcomes. Potential sources of bias in the lipidomics analyses include the type and status of the underlying disease, serum labile iron levels, prior chemotherapy or medication exposure, unidentified confounding factors, and differences in sample collection or storage time. However, given the major influence of albumin levels on the antifungal activity of serum and on the abundance

of oxidized free fatty acids (FFAs), together with the validation of human findings in albumin-deficient humanized mouse models, it is unlikely that other confounders had a major impact on the results of our study.

Ethics oversight

The study at the Leukemia Department of the MD Anderson Cancer Center was approved by the IRB (IRB Protocol: PA14-0802) of the MDACC.

The study was approved by the Institutional Ethics Committee (IEC; Intramural; INT) of the PGIMER;(IEC/INT approval no: 2023/Study-1564) and registered with the Biological Research Regulatory Approval Portal (BIORRAP; registration no. POS36452025). All procedures were conducted in accordance with institutional and national guidelines and regulations.

The studies at the University Hospital of Heraklion, Crete, and the Therapeutics Clinic of the General Hospital of Athens "Alexandra" were approved by the IRBs of the corresponding hospitals. Specifically, approval for the collection of clinical information and blood samples from all individuals mentioned above was obtained from the Ethics Committee of the University of Heraklion, Crete, Greece (5159/2014, 10925/201 and 13-04-22/7970) and the Therapeutics Clinic (122/18-2-2021). All patients were fully informed and provided written informed consent in accordance with the Declaration of Helsinki.

For lipidomic and functional studies, serum samples from patients with mucormycosis or invasive pulmonary aspergillosis, and matched control patients, were obtained from hematological malignancy patients admitted to the University Hospitals of Leuven, Belgium (IRB# S61797).

Note that full information on the approval of the study protocol must also be provided in the manuscript.

Field-specific reporting

Please select the one below that is the best fit for your research. If you are not sure, read the appropriate sections before making your selection.

☒ Life sciences ☐ Behavioural & social sciences ☐ Ecological, evolutionary & environmental sciences

For a reference copy of the document with all sections, see nature.com/documents/nr-reporting-summary-flat.pdf

Life sciences study design

All studies must disclose on these points even when the disclosure is negative.

Sample size	Sample sizes of at least five per group were chosen as this would allow the detection of a 25% difference in the mean between experimental and control groups with a probability of greater than 95% ($p < 0.05$), assuming a standard deviation of around 15% and a minimum power value of 0.8. The sample size for our in vivo/animal studies was determined based on pilot studies performed at the beginning of the project. The minimum necessary number of mice was used according to the international guidelines for animal research and the 3 Rs principle.
Data exclusions	No data were excluded from our analyses.
Replication	All experiments were independently replicated at least twice unless otherwise indicated in the manuscript. Our sample size secured experimental reproducibility. Individual data points, presented as dots, are shown in the figures and numbers of biological replicates (n) are indicated in the figure legends.
Randomization	Animals used in each experiment were age- and sex-matched and, whenever possible, housed in the same cage. Mice were randomly allocated to experimental groups in all experiments. In addition, fungal, murine, and human sample groups were randomly assigned in all in vitro assays.
Blinding	Mouse histopathology and imaging analyses were evaluated in a blinded manner by at least two researchers. Lung fungal loads were assessed independently and blinded by an experienced pathologist (E.D.). All other experiments were not blinded, as the investigator who planned the experiments, also performed them but were conducted according to standardized protocols and procedures.

Reporting for specific materials, systems and methods

We require information from authors about some types of materials, experimental systems and methods used in many studies. Here, indicate whether each material, system or method listed is relevant to your study. If you are not sure if a list item applies to your research, read the appropriate section before selecting a response.

Materials & experimental systems

n/a	Involved in the study
☐	☒ Antibodies
☐	☒ Eukaryotic cell lines
☒	☐ Palaeontology and archaeology
☐	☒ Animals and other organisms
☒	☐ Clinical data
☒	☐ Dual use research of concern
☒	☐ Plants

Methods

n/a	Involved in the study
☒	☐ ChIP-seq
☐	☒ Flow cytometry
☒	☐ MRI-based neuroimaging

Antibodies

Antibodies used

Primary antibodies:
Rabbit anti-mucoricin antibody was generated as previously described (Soliman S.S.M. et al., Nat. Microbiol. 2021)
Rabbit anti-CotH3 antibody was generated as previously described (Gebremariam, T. et al., J Clin Invest 2010)
Briefly, rabbit antibodies against recombinant CotH3 and mucoricin coupled to KLH were raised by ProMab Biotechnologies Inc. The IgG fraction was purified from the antisera using protein A/G spin columns (Thermo Fisher Scientific) according to the manufacturer's instructions.
Mouse anti-transferrin antibody (D-9), Santa Cruz, sc-365871
Goat anti-albumin antibody (P-20), Santa Cruz, sc-46293
Rabbit anti-cleaved Caspase-3 (Asp175) antibody, Cell Signaling, #9661

Secondary antibodies:
Anti-mouse IgG, HRP-linked antibody, Cell Signaling, #7076
Donkey anti-goat IgG, HRP-conjugated antibody, Sigma-Aldrich, AP180P
Goat anti-rabbit CF488A antibody, Biotium, 20012
Goat anti-rabbit CF555 antibody, Biotium, 20033

Validation

Rabbit anti-mucoricin antibody was verified by ELISA, Western blots and immunofluorence assays as detailed in Soliman S.S.M. et al., Nat. Microbiol. 2021.
Rabbit anti-CotH3 antibody was verified by Flow cytometry and immunofluorence assays as detailed in Gebremariam, T. et al., J Clin Invest 2010.
All other antibodies were quality control tested and application validated by their respective manufacturer.
Specifically: Mouse anti-transferrin antibody (D-9) is recommended for detection of transferrin of human origin by Western Blotting (https://datasheets.scbt.com/sc-365871.pdf).
Goat anti-albumin antibody (P-20) is recommended for detection of albumin of human origin by Western Blotting (https://datasheets.scbt.com/sc-46293.pdf).
Rabbit anti-cleaved Caspase-3 antibody (Asp175) is recommended for detection of activated caspase-3 of mouse origin by Immunohistochemistry (Paraffin) (https://media.cellsignal.com/coa/9661/47/9661-lot-47-coa.pdf).

Eukaryotic cell lines

Policy information about cell lines and Sex and Gender in Research

Cell line source(s)

Human alveolar epithelial cells (A549 cells) were obtained from a 58-year-old male Caucasian patient with carcinoma and procured from the American Type Culture Collection (ATCC). Primary alveolar epithelial cells were obtained from ScienCell (cat. no. 3200), propagated in Alveolar Epithelial Cell medium (cat. no. 3201) and passaged once.

Authentication

A549 have been purchased from ATCC. Both cell types were authenticated morphologically

Mycoplasma contamination

A549 cells were routinely tested for Mycoplasma contamination with negative results.

Commonly misidentified lines
(See ICLAC register)

None is listed as misidentified

Animals and other research organisms

Policy information about studies involving animals; ARRIVE guidelines recommended for reporting animal research, and Sex and Gender in Research

Laboratory animals

C57BL/6 and B6.Cg-Tg(FCGRT)32Dcr Albem12Mvw Fcgrttm1Dcr/MvwJ mice (in C57BL/6 background) were purchased from The Jackson Laboratory. All mice were maintained at IMBB/FORTH's specific pathogen-free facility , in grouped cages in a high-efficiency air-filtered, environmentally controlled, virus-free facility (24°C, 50–60% relative humidity, 12/12 h light/dark cycle) and fed a standard chow diet and water ad libitum. In all experiments 8-12-week-old, sex-matched mice were used. Mice from different experimental groups, including transgenic and their WT counterparts, were housed in the same cage to limit the impact of inter-individual microbiota on the variability of the experimental outcome.

Wild animals	The study did not involve wild animals.
Reporting on sex	Mice of both sexes were included in the study and since the outcome of infection with R. delemar was similar in both sexes, no sex-based analyses were performed.
Field-collected samples	The study did not involve samples collected from the field.
Ethics oversight	All experiments were approved by the local Ethics Committee of the University of Crete Medical School, the FORTH Ethics Committee, and the Directorate of Agricultural and Veterinary Policy of the Region of Crete, in accordance with national and European Union legislation (animal protocols 17/07/2017-147075 and 22/03/2023-90477). All efforts were made to minimize the number of animals used and their suffering

Note that full information on the approval of the study protocol must also be provided in the manuscript.

Plants

Seed stocks	*Report on the source of all seed stocks or other plant material used. If applicable, state the seed stock centre and catalogue number. If plant specimens were collected from the field, describe the collection location, date and sampling procedures.*
Novel plant genotypes	*Describe the methods by which all novel plant genotypes were produced. This includes those generated by transgenic approaches, gene editing, chemical/radiation-based mutagenesis and hybridization. For transgenic lines, describe the transformation method, the number of independent lines analyzed and the generation upon which experiments were performed. For gene-edited lines, describe the editor used, the endogenous sequence targeted for editing, the targeting guide RNA sequence (if applicable) and how the editor was applied.*
Authentication	*Describe any authentication procedures for each seed stock used or novel genotype generated. Describe any experiments used to assess the effect of a mutation and, where applicable, how potential secondary effects (e.g. second site T-DNA insertions, mosiacism, off-target gene editing) were examined.*

Flow Cytometry

Plots

Confirm that:

☒ The axis labels state the marker and fluorochrome used (e.g. CD4-FITC).

☒ The axis scales are clearly visible. Include numbers along axes only for bottom left plot of group (a 'group' is an analysis of identical markers).

☒ All plots are contour plots with outliers or pseudocolor plots.

☒ A numerical value for number of cells or percentage (with statistics) is provided.

Methodology

Sample preparation	R. delemar spores were cultured in 5% ethanol/RPMI-MOPS supplemented with oleic acid (Sigma-Aldrich) or oxidized oleic acid at 37oC for 5 hours. The spores were harvested with scraping, collected in low affinity 1.5ml tubes, washed twice with PBS and fixed with methanol-free 4% formaldehyde at RT for 20mins. Subsequently, the spores were washed twice with PBS, stained with 0.5 μg/ml Nile Red (Thermo Fisher Scientific) at RT for 20mins, washed again twice with PBS and stained with 200 μg/ml Calcofluor White (CFW) at RT for 20mins.
Instrument	BD Biosciences, FACSCanto II system.
Software	BD Sciences, FlowJo v10.6 Software.
Cell population abundance	Analysis of Nile Red emission intensity was performed in R.delemar spores, hence the cell population purity was 100%.
Gating strategy	Whole fungal cell fragment was gated in FSC-A/SSC-A and single cells were gated in FSC-H/FSC-A plot. Live, CFW positive spores were selected and Nile Red uptake was depicted in histogram plots.

☒ Tick this box to confirm that a figure exemplifying the gating strategy is provided in the Supplementary Information.